LEVEL II

①

UNITED STATES AIR FORCE
AIR UNIVERSITY
AIR FORCE INSTITUTE OF TECHNOLOGY
Wright-Patterson Air Force Base, Ohio

82 02 18 131

OPTIMAL CONTROL USING FREQUENCY

WEIGHTED COST FUNCTIONALS

THESIS

AFIT/GAE/AA/81D-22   D. V. Palmer
                      Capt   USAF

OPTIMAL CONTROL USING

FREQUENCY WEIGHTED COST FUNCTIONALS

THESIS

Presented to the Faculty of the School of Engineering

of the Air Force Institute of Technology

Air University

in Partial Fulfillment of the

Requirements for the Degree of

Master of Science

by

D. V. Palmer, B.S.A.E.

Captain   USAF

Graduate Aeronautical Engineering

December 1981

Preface

This thesis is an investigation in a discipline which is of special interest to me academically and professionally. Control systems advancements are beneficial in many areas of aeronautical, electrical, and mechanical engineering.

I would like to give special thanks to Dr. Robert Calico, Jr. and Dr. James Silverthorn for their constant support, motivation, and guidance on this project. I would also like to thank my typist, Gloria Miller, for her patience and professionalism.

Table of Contents

Contents

List of Figures

List of Tables

List of Symbols

a = weighting parameter

$\underline{A}$ = open-loop plant matrix

$\underline{\tilde{A}}$ = open-loop augmented plant matrix

$\underline{\tilde{A}}_{CL}$ = closed-loop augmented plant matrix

$\underline{A}_1$ = state controller plant matrix

$\underline{A}_2$ = control regulator plant matrix

b = weighting parameter

$\underline{B}$ = open-loop control matrix

$\underline{\tilde{B}}$ = augmented control matrix

$\underline{B}_1$ = state controller control matrix

$\underline{B}_2$ = control regulator control matrix

$\underline{C}$ = open-loop output matrix

$\underline{\tilde{C}}$ = augmented output matrix

$\underline{C}_1$ = state regulator output matrix

$\underline{C}_2$ = control regulator output matrix

$\underline{D}$ = open-loop feed forward matrix

$\underline{\tilde{D}}$ = augmented feed forward matrix

$\underline{D}_1$ = state controller feed forward matrix

$\underline{D}_2$ = control regulator feed forward matrix

$\underline{G}$ = system transfer function matrix

$\underline{H}$ = system transfer function matrix

$\underline{I}$ = identity matrix

J = performance index

J_{ss} = steady state performance index

$\underline{K}$ = Riccati feedback gain matrix

Symbols

$\underset{\sim}{\underline{K}}$ = augmented Riccati feedback gain matrix

$\underline{K}_x$ = state feedback gain vector

$\underline{K}_z$ = controller feedback gain vector

m = order of control

n = order of system

P_i = transfer function polynomial coefficient

$\underline{P}_1$ = transfer function between $\underline{x}^1$ and $\underline{x}$

$\underline{P}_2$ = transfer function between $\underline{u}^1$ and $\underline{u}$

$\underline{Q}_i$ = transfer function coefficient matrix

r = arbitrary input

s = Laplace variable

$\underline{S}$ = Riccati matrix

$\underset{\sim}{\underline{S}}$ = augmented Riccati matrix

t = time

t_p = peak time

t_s = settling time

$\underline{u}$ = control vector

$\underline{u}^1$ = frequency shaped control vector

$\underline{u}^*$ = optimal control vector

$\underline{u}_c$ = commanded control vector

$\underline{x}$ = state vector

$\underset{\sim}{\underline{x}}$ = augmented state vector

$\underline{x}^1$ = frequency shaped state vector

$\underline{y}$ = output vector

$\underline{z}_1$ = state vector for state controller

Symbols

$\underline{z}_2$ = state vector for control regulator

ζ = damping ratio

ω = frequency

ω_n = natural frequency

Abstract

A simple lightly damped second-order system is augmented with an optimal controller using linear quadratic regulator theory. However, instead of using conventional optimal control design methods, the controller is designed with frequency weighted cost functionals. This report investigates the effect of frequency shaping on the frequency and time response characteristics of the closed-loop system.

The effects of frequency shaping on the state and control penalty matrices are analyzed separately. Each test case yields improved damping ratios compared with the baseline open-loop system. Each system, including the baseline model, has a high frequency asymptote slope of -40 dB/decade. There is very little difference in the high-frequency response characteristics of the frequency shaped augmented systems and the open-loop system.

The most important result is that the low frequency magnitude response can be reduced by using frequency shapings. This is particularly useful in attenuating low frequency system modes as well as low frequency noise.

OPTIMAL CONTROL USING
FREQUENCY WEIGHTED COST FUNCTIONALS

I   Introduction

Control system design has typically involved either
frequency domain compensation or state space time domain
techniques. Using frequency domain analysis techniques,
control systems designers have developed an understanding
and an intuition for what type of frequency response
characteristics a system should have. The design tech-
nique is then to add compensation in such a manner so as
to obtain this desired frequency response.

An advantage of frequency domain analysis is that
there exists a great body of knowledge concerning this
method. For example, the use of washout circuits in
aircraft yaw dampers is very common, very effective, and
done purely in the frequency domain.

A significant disadvantage to frequency domain
analysis, which is discussed in Ch. 2, is that it is dif-
ficult to apply the method to multiple-input-multiple-
output (MIMO) systems.

State space techniques differ in that they deal
directly with the time domain characteristics of the
system. A common state space technique is the use of
linear quadratic optimal control. The designer defines
a quadratic cost functional and then by minimizing the
cost functional determines the optimal control. One main

advantage to the state space method, discussed in Ch. 2, is the ease at which it can be applied to MIMO systems through the use of vector and matrix representations. Optimal control design generally requires choosing constant weighting matrices for the cost functional.

There has been much research on determining the control of a system using both the frequency domain and time domain systems. However, it is not clear what advantages might be gained by using some combination of the two methods.

Background

Recent work by N. K. Gupta (Refs 6,7) has shown that optimal control theory can also be applied to cost functionals involving frequency dependent weighting matrices. Gupta suggests that this method is very helpful in controlling spillover, reducing high frequency response, and improving disturbance rejection (Ref 6). It is currently known how to formulate this problem, but Gupta has not shown or suggested any relationship between the cost functionals and the frequency response of the closed-loop system.

Problem

The problem is to investigate the relationship between these frequency weighted cost functionals and the conventional frequency response analysis techniques.

Specifically, frequency response characteristics such as magnitude overshoot, high frequency asymptote slope, break frequency, and damping are examined. Additionally, time response characteristics of the systems are examined.

Assumptions

It is assumed that all system models are linear deterministic, that is, that the systems are noise-free.

General Approach

Using a simple plant, several frequency shaped cost functionals proposed by Gupta are analyzed.

The closed-loop response of a second order baseline system with no controller is analyzed. Then the baseline system is augmented with a baseline controller. Subsequent cases examine the closed-loop response of the baseline system augmented with Gupta's suggested frequency weighted controllers. The frequency weighted controllers are compared with the baseline controllers in terms of frequency and time response. The effect of frequency shapings on both the state and the control penalty matrices is examined.

II Theoretical Development

Many feedback control systems can be designed using the linear time invariant system model

$$\dot{\underline{x}}(t) = \underline{A}\underline{x}(t) + \underline{B}\underline{u}(t) \quad \underline{x}(o) = \underline{x}_o \quad (o \leq t \leq t_f) \qquad (2\text{-}1)$$

$$\underline{y}(t) = \underline{C}\underline{x}(t) + \underline{D}\underline{u}(t) \qquad (2\text{-}2)$$

where $\underline{x}$ is an n-dimensional state vector, $\underline{u}$ is an m-dimensional control vector, $\underline{y}$ is a p-dimensional output vector, $\underline{A}$ is an n x n plant matrix, $\underline{B}$ is an n x m control matrix, $\underline{c}$ is a p x n output matrix, and $\underline{D}$ is a p x m feed-forward matrix.

The control, $\underline{u}$, can be defined to be the product of a constant feedback matrix, $\underline{K}$, and the state vector, $\underline{x}(t)$, in the following manner:

$$\underline{u}(t) = -\underline{K}\underline{x}(t) \qquad (2\text{-}3)$$

There are various methods of determining the feedback gain matrix, $\underline{K}$. Pole placement techniques, entire eigen-structure assignment, steady state solution of appropriate Riccati equations via linear quadratic methodology, and even arbitrary selection are some of these methods. The value of $\underline{K}$ is manipulated until the desired closed-loop system dynamics are achieved. Fig. 2-1 shows a block diagram of the closed-loop system where $\underline{r}$ is an arbitrary input. It $\underline{r}$ is assumed to be a constant value other than zero and the feedback $\underline{u}(t) = -\underline{K} \quad \underline{x}(t) + \underline{r}(t)$ is used, the state equation for the closed-loop system becomes

4

$$\dot{\underline{x}}(t) = \underline{A}\underline{x}(t) + \underline{B}\underline{u}(t) = (\underline{A} - \underline{B}\underline{K})\underline{x}(t) + \underline{B}\underline{r}(t) \quad (2\text{-}4)$$

where $\underline{u}(t) = \underline{r}(t) - \underline{K}\underline{x}(t)$. The poles of the system transfer function between $\underline{x}(t)$ and $\underline{u}(t)$ are the eigenvalues of $(\underline{A} - \underline{B}\ \underline{K})$.

Optimal Control Methods

Using linear optimal theory, the control $\underline{u}(t)$ is chosen so that it minimizes the quadratic performance index

$$J = \int_{0}^{t_f} \{\underline{x}^T(t)\ \underline{Q}\underline{x}(t) + \underline{u}^T(t)\ \underline{R}\underline{u}(t)\}dt + \underline{x}^T(t_f)\underline{S}_f\underline{x}(t_f) \quad (2\text{-}5)$$

where $\underline{Q}$ is a time invariant positive semidefinite state penalty matrix, $\underline{R}$ is a time invariant positive definite control penalty matrix, and $\underline{S}_f = \underline{S}(t_f)$. This process yields a time invariant feedback gain matrix, $\underline{K}$.

The optimal control, $\underline{u}^*(t)$, is defined as

$$\underline{u}^*(t) = -\underline{K}\ \underline{x}(t) \quad (2\text{-}6)$$

The feedback control gain matrix $\underline{K}$ is determined by the solution to the Riccati equation:
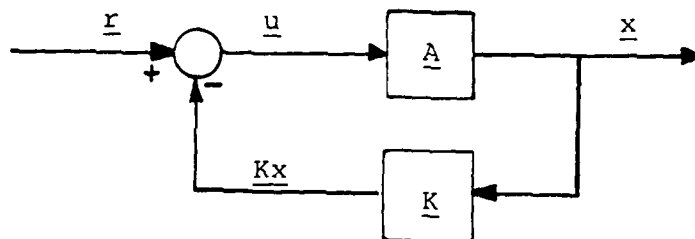
Fig. 2-1. Closed-Loop System

5

$$\underline{\dot{S}} = \underline{A}^T\underline{S} + \underline{SA} + \underline{Q} - \underline{SBR}^{-1}\underline{B}^T\underline{S} \quad \underline{S}(t_f) = \underline{S}_f \qquad (2\text{-}7)$$

$$\underline{K} = \underline{R}^{-1}\,\underline{B}^T\,\underline{S} \qquad (2\text{-}8)$$

Therefore, the optimal control law is a function of the
matrices $\underline{A}$ and $\underline{B}$ defined in the linear system model, and
of the matrices $\underline{Q}$, $\underline{R}$, and $\underline{S}_f$, defined in the quadratic
performance index. If the system is both detectable and
stabilizable, then as the system reaches steady state (i.e.,
as $t \to \infty$) the solution to the Riccati Eq (2-7) converges
to a constant, steady state value regardless of $\underline{S}_f$. This
solution is determined by setting $\underline{\dot{S}} = \underline{0}$. Thus, from
Eq (2-8) it is clear that the Riccati feedback gain matrix,
$\underline{K}$, also becomes a constant and the optimal control law,
Eq (2-6), becomes time invariant in steady state (Ref 5:
574-5). Therefore, the last term of the quadratic per-
formance index, Eq (2-5), becomes negligible at large
enough values of time, t. The term is assumed to be zero,
yielding the steady state quadratic performance index

$$J_{ss} = \int_0^\infty \{\underline{x}^T(t)\,\underline{Q}\,\underline{x}(t) + \underline{u}(t)^T\underline{R}\,\underline{u}(t)\}\,dt \qquad (2\text{-}9)$$

There is no clearly defined method for choosing the
penalty matrices $\underline{Q}$ and $\underline{R}$. Typically, $\underline{Q}$ and $\underline{R}$ are
initially chosen to be diagonal matrices with each
diagonal element equal to the reciprocal of the maximum
allowable excursion squared. Then $\underline{Q}$ and $\underline{R}$ must be tuned
to achieve the desired response. The tuning procedure
is fairly arbitrary and usually done by engineering

intuition. In general, the process is an iterative one
with the following steps:

1. Choose values for $\underline{Q}$ and $\underline{R}$

2. Determine the Riccati feedback gain matrix, $\underline{K}$

3. Determine the closed-loop state matrix, $(\underline{A}-\underline{B}\underline{K})$

4. Determine the frequency response and/or time
   response characteristics of the system

5. Repeat steps 1 through 4 until the system has
   the desired response characteristics

The larger the value of a particular term in the $\underline{Q}$ matrix,
the more that particular state value will be penalized for
deviation from some desired nominal trajectory. Similarly,
the larger the value of the $\underline{R}$ matrix, the larger the
penalty for using excessive control.

Classical Control Methods

Classical control methods typically use frequency
domain models and analysis techniques in the design and
compensation of control systems. These methods use the
transfer function between the input, u, and the output,
y, that is:

$$G(s) = y(s)/u(s) \qquad (2\text{-}10)$$

where G(s) is the transfer function matrix and

$$G_{ij}(s) = y_i(s)/u_j(s). \qquad u_k(s) = 0, k \neq j \qquad (2\text{-}11)$$

Classical techniques typically include the root-locus
method, Bode-plot representations, Nyquist diagrams, and

7

Nichols charts to assist the designer in giving a system the specified response characteristics. Unfortunately, these methods are mostly limited to single-input-single-output (SISO) systems, and cannot easily be used for multiple-input-multiple-output (MIMO) systems. In the MIMO system case, as one transfer function is compensated, it affects others and designing a control system using classical methods becomes increasingly more difficult, especially for coupled off-diagonal terms. Optimal control design methods, using vector mathematics, are much more suited to the MIMO systems. Linear quadratic regulators have an advantage that the controller is guaranteed to be stable with 60° phase margin and 50% to infinite gain margin. A disadvantage of classical methods is that the designer must be careful to insure that the system is stable.

Frequency Shaping of Cost Functionals

Gupta (6:5) has suggested that optimal control theory can also be applied to cost functionals involving frequency dependent state and control penalty matrices, $\underline{Q}$ and $\underline{R}$, respectively.

Gupta states that some of these controllers behave like lag compensators, and that they reduce the high frequency response of the system. However, the frequency dependent penalty matrices cannot be mixed outright with the time dependent state and control variables in the performance index (Eq 2-9). Therefore the steady state

quadratic performance index is written initially in the frequency domain in the following manner:

$$J = \int_{-\infty}^{\infty} \{ \underline{x}^*(j\omega)\underline{Q}(\omega)\underline{x}(j\omega) + \underline{u}^*(j\omega)\underline{R}(\omega)\underline{u}(j\omega) \} d\omega \qquad (2\text{-}12)$$

where the asterisk, *, means complex conjugate transpose, and the $\underline{Q}(\omega)$ and $\underline{R}(\omega)$ state and control penalty matrices, respectively, are specified to be Hermitian positive semi-definite and Hermitian positive definite, respectively. Once the frequency domain performance index is defined, it is transformed to the more readily usable time domain performance index using Parseval's Theorem. That is, the performance index is evaluated by using the time domain performance index transformed from the specified frequency domain performance index. The Riccati matrix feedback gain is calculated, which, in turn, gives the optimal control, $\underline{u}^*$, for the closed loop system. The closed-loop plant matrix, $\underline{A}_{CL} = (\underline{A} - \underline{B}\,\underline{K})$, is used to analyze the closed-loop performance of the system.

Control Law Design

Having defined the frequency domain performance index (Eq 2-12), the next step is to factor the terms $\underline{x}^*(j\omega)\underline{Q}(\omega)\underline{x}(j\omega)$ and $\underline{u}^*(j\omega)\,\underline{R}(\omega)\underline{u}(j\omega)$ into the terms $\underline{x}^{1*}(j\omega)$ $\underline{x}^1(j\omega)$ and $\underline{u}^{1*}(j\omega)\underline{u}^1(j\omega)$ respectively where

$$\underline{x}^1(j\omega) = \underline{P}_1(j\omega)\underline{x}(j\omega) \qquad (2\text{-}13)$$

$$\underline{u}^1(j\omega) = \underline{P}_2(j\omega)\underline{u}(j\omega) \qquad (2\text{-}14)$$

9

and

$$\underline{P}_1{}^*(j\omega)\ \underline{P}_1(j\omega)\ =\ \underline{Q}(j\omega) \qquad (2\text{-}15)$$

$$\underline{P}_2{}^*(j\omega)\ \underline{P}_2(j\omega)\ =\ \underline{R}(j\omega) \qquad (2\text{-}16)$$

The pair of matrices $\underline{P}_1{}^*(j\omega)$ and $\underline{P}_1(j\omega)$ and the pair $\underline{P}_2{}^*(j\omega)$ and $\underline{P}_2(j\omega)$ are complex conjugate transpose matrices. The following relationship exists between $\underline{x}(j\omega)$ and $\underline{x}^1(j\omega)$:

$$\underline{x}(j\omega) \longrightarrow \boxed{\underline{P}_1(j\omega)} \longrightarrow \underline{x}^1(j\omega)$$
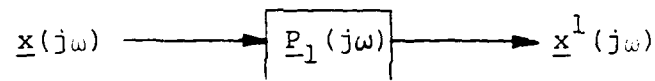
That is, we get $x^1(j\omega)$ by putting $\underline{x}(j\omega)$ through a linear system, $\underline{G}_x(j\omega)$, whose frequency response is described by the transfer function matrix $\underline{P}_1(j\omega)$, i.e.,

$$\underline{G}_x(j\omega)\ =\ \underline{P}_1(j\omega) \qquad (2\text{-}17)$$

This spectral factorization of $\underline{Q}(\omega)$ and $\underline{R}(\omega)$ is necessary to facilitate the Fourier transformation of the frequency domain performance index into the time domain. That is,

$$\underline{Q}(\omega)\ =\ \underline{P}_1{}^*(j\omega)\ \underline{P}_1(j\omega) \qquad (2\text{-}18)$$

$$\underline{R}(\omega)\ =\ \underline{P}_2{}^*(j\omega)\ \underline{P}_2(j\omega) \qquad (2\text{-}19)$$

and

$$J\ =\ \int_{-\infty}^{\infty} \{\underline{x}^*(j\omega)\ \underline{P}_1{}^*(j\omega)\ \underline{P}_1(j\omega)\ \underline{x}(j\omega)$$
$$+\ \underline{u}^*(j\omega)\ \underline{P}_2{}^*(j\omega)\ \underline{P}_2(j\omega)\ \underline{u}(j\omega)\}\ d\omega \qquad (2\text{-}20)$$

Therefore the performance index becomes

$$J = \int_{-\infty}^{\infty} \{ \underline{x}^{1*}(j\omega) \; \underline{I} \; \underline{x}^1(j\omega) + \underline{u}^{1*}(j\omega) \; \underline{I} \; \underline{u}^1(j\omega) \} d\omega \qquad (2\text{-}21)$$

where $\underline{x}^{1*}$, $\underline{x}^1$, and the first $\underline{I}$ are n x n matrices and $\underline{u}^{1*}$, $\underline{u}^1$, and the second $\underline{I}$ are m x m matrices. Using the inverse Fourier transformation, Eq (2-21) can be written equivalently in the time domain as the following:

$$J = \int_0^{\infty} \{ \underline{x}^{1T}(t) \; \underline{I} \; \underline{x}^1(t) + \underline{u}^{1T}(t) \; \underline{I} \; \underline{u}^1(t) \} dt \qquad (2\text{-}22)$$

Using the relation of Eq (2-13), an equivalent model of the system can be described by the following differential equations with output $\underline{x}^1$, state $\underline{z}_1$, and input $\underline{x}$.

$$\underline{\dot{z}}_1(t) = \underline{A}_1 \underline{z}_1(t) + \underline{B}_1 \underline{x}(t) \qquad (2\text{-}23)$$

$$\underline{x}^1(t) = \underline{C}_1 \underline{z}_1(t) + \underline{D}_1 \underline{x}(t) \qquad (2\text{-}24)$$

The feed-forward matrix, $\underline{D}_1$, is zero if $\underline{P}_1(j\omega)$ is proper, that is, if the degree of the $\underline{P}_1(j\omega)$ numerator is of smaller order than the $\underline{P}_1(j\omega)$ denominator. Eqs (2-23) and (2-24) model the augmented system which includes the original states and the frequency weightings of the controller. Appendix D illustrates the use of the $\underline{D}_1$ matrix. A similar relation exists for the control relation described in Eq (2-14) with output $\underline{u}^1$, state $\underline{z}_2$, and input $\underline{u}$:

$$\underline{\dot{z}}_2(t) = \underline{A}_2 \underline{z}_2(t) + \underline{B}_2 \underline{u}(t) \qquad (2\text{-}25)$$

$$\underline{u}^1(t) = \underline{C}_2 \underline{z}_2(t) + \underline{D}_2 \underline{u}(t) \qquad (2\text{-}26)$$

11

Fig. 2-2 shows a block diagram of the generalized controller (Ref 5:531). Therefore the entire system dynamics can be described by the following:

$$\frac{d}{dt}\begin{bmatrix} \underline{x}(t) \\ \underline{z}_1(t) \\ \underline{z}_2(t) \end{bmatrix} = \begin{bmatrix} \underline{A} & \underline{0} & \underline{0} \\ \underline{B}_1 & \underline{A}_1 & \underline{0} \\ \underline{0} & \underline{0} & \underline{A}_2 \end{bmatrix} \begin{bmatrix} \underline{x}(t) \\ \underline{z}_1(t) \\ \underline{z}_2(t) \end{bmatrix} + \begin{bmatrix} \underline{B} \\ \underline{0} \\ \underline{B}_2 \end{bmatrix} \underline{u}(t) \qquad (2\text{-}27)$$

Eq (2-27) can be defined in terms of the following new variables and matrices:

$$\frac{d}{dt}\ \underline{\tilde{x}}(t) = [\underline{\tilde{A}}]\underline{\tilde{x}}(t) + [\underline{\tilde{B}}]\underline{u}(t) \qquad (2\text{-}28)$$

The new steady state performance index becomes:

$$J_{ss} = \int_0^\infty \{\underline{\tilde{x}}^T(t)\underline{\tilde{Q}}\underline{\tilde{x}}(t) + \underline{u}^T(t)\underline{\tilde{R}}\underline{u}(t)\}dt \qquad (2\text{-}29)$$

where $\underline{\tilde{Q}}$ and $\underline{\tilde{R}}$ are the state and control penalty matrices, respectively, formed from the augmented system defined in Eqs (2-23) through (2-26). Eq (2-29) can be written in matrix notation to be the following:

$$J_{ss} = \int_0^\infty [\underline{\tilde{x}}^T(t)\ \ \underline{u}^T(t)]\begin{bmatrix} \underline{\tilde{Q}} & \underline{0} \\ \underline{0} & \underline{\tilde{R}} \end{bmatrix}\begin{bmatrix} \underline{\tilde{x}}(t) \\ \underline{u}(t) \end{bmatrix} \qquad (2\text{-}30)$$

or equivalently:

$$J_{ss} = \int_0^\infty [\underline{x}^T(t),\underline{z}_1^T(t),\underline{z}_2^T(t),\underline{u}^T(t)]\begin{bmatrix} \underline{D}_1^T\underline{D}_1 & \underline{D}_1^T\underline{C}_1 & \underline{0} & \underline{0} \\ \underline{C}_1^T\underline{D}_1 & \underline{C}_1^T\underline{C}_1 & \underline{0} & \underline{0} \\ \underline{0} & \underline{0} & \underline{C}_2^T\underline{C}_2 & \underline{C}_2^T\underline{D}_2 \\ \underline{0} & \underline{0} & \underline{D}_2^T\underline{C}_2 & \underline{D}_2^T\underline{D}_2 \end{bmatrix}\begin{bmatrix} \underline{x}(t) \\ \underline{z}_1(t) \\ \underline{z}_2^T(t) \\ \underline{u}(t) \end{bmatrix}dt$$

$$(2\text{-}31)$$

12
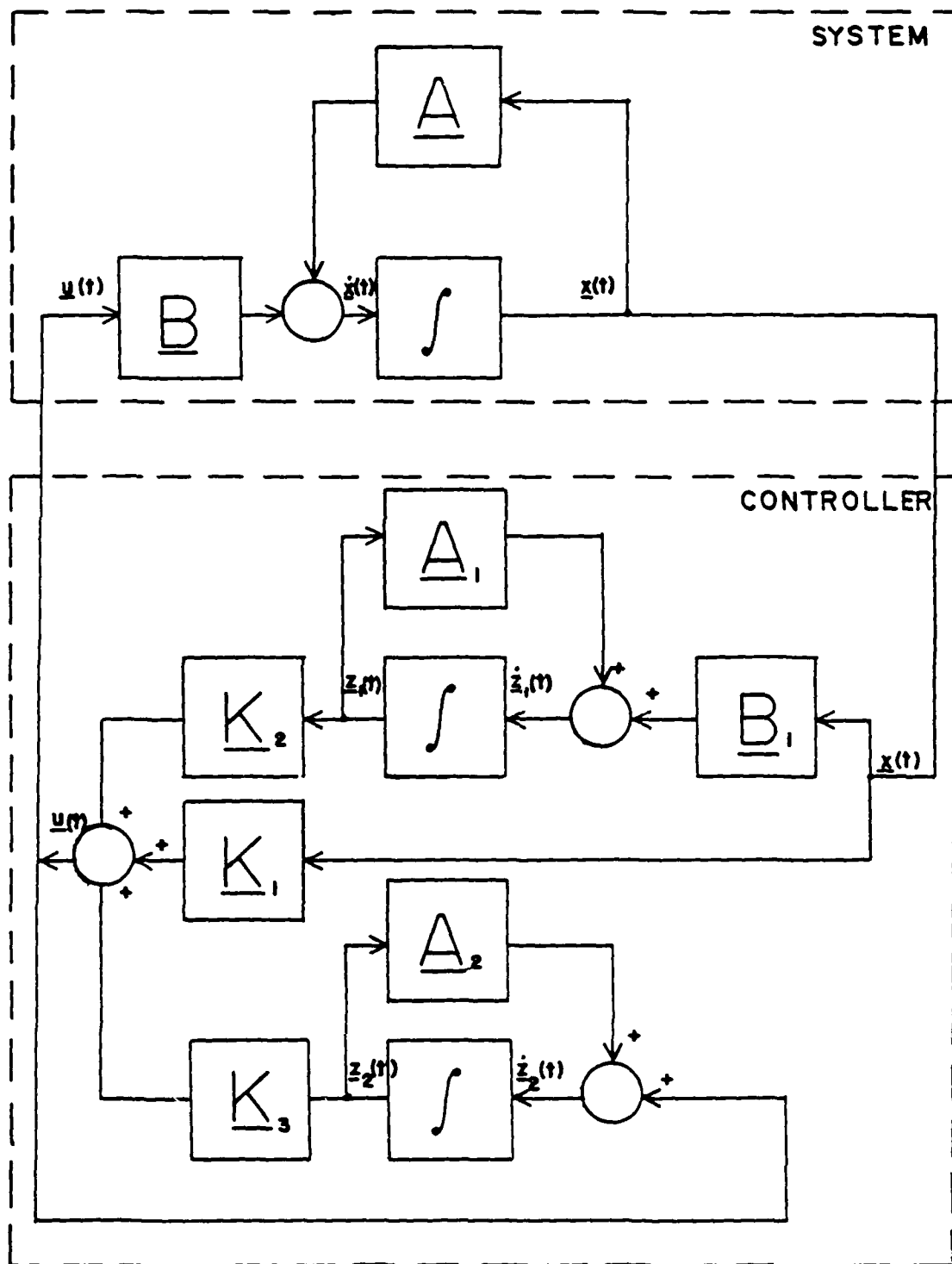
Fig. 2-2. Block Diagram of Generalized Controller

13

Solving Eqs (2-27) and (2-31) in the steady state Riccati Equation yelds $\tilde{\underline{S}}$ which defines the Riccati feedback gain matrix $\tilde{\underline{K}}$ for the augmented system. The optimal control for the augmented system is defined to be:

$$\underline{u}^*(t) = \tilde{\underline{K}} \, \tilde{\underline{x}}(t) = \underline{K}_x \, \underline{x} + \underline{K}_{z_1} \, \underline{z}_1 + \underline{K}_{z_2} \, \underline{z}_2 \qquad (2\text{-}32)$$

The scope of this report is limited to the analysis of the time response and Bode frequency response characteristics of the closed-loop system.

III   Computer Programs and Methods

Once the theory of incorporating frequency weighted cost functionals is established, it is necessary to implement the closed-loop augmented system in some readily usable manner. The synthesis of the new system is done with the use of digital computer programs. The use of these programs is described in this section.

Use of OPTCON Program

Having defined the augmented system matrices $\tilde{A}$, $\tilde{B}$, $\tilde{Q}$, and $\tilde{R}$ the first step in analyzing the augmented system is to calculate the Riccati matrix feedback gain, $\tilde{K} = [K_x, K_{z_1}, K_{z_2}]$. There are currently several programs which solve the steady state Riccati equation. The program MRIC by Kleinman (Ref 9) can be used with other subroutines to multiply, add, invert, and transpose matrices to solve the Riccati equation. The program OPTCON (Ref 14) is an interactive program for optimal control analysis that incorporates MRIC and these other matrix operator subroutines to solve the Riccati equation. The new system matrices $\tilde{A}$ and $\tilde{B}$ and the penalty matrices $\tilde{Q}$ and $\tilde{R}$ are entered into OPTCON. OPTCON will output the Riccati solution, Riccati feedback gain matrix, $\tilde{K}$, and the closed-loop eigenvalues.

Use of TOTAL Program

Once the Riccati feedback gain matrix, $\tilde{K}$, is determined, the new closed-loop system plant matrix, $\tilde{A}_{CL}$, is

15

formed as $\tilde{\underline{A}}_{CL} = (\tilde{\underline{A}} - \tilde{\underline{B}}\tilde{\underline{K}})$. Now the Bode frequency response
and time response of the closed-loop system is analyzed
using the interactive program TOTAL (Ref 9). The $\tilde{\underline{A}}_{CL}$, $\tilde{\underline{B}}$,
$\tilde{\underline{C}}$, and $\tilde{\underline{D}}$ matrices are input and the closed-loop transfer
function of the new system is calculated. Then the Bode
frequency response characteristics and the time response
characteristics of each system can be analyzed. This
process is repeated for each of the various cases to
determine any advantages of one controller over the
others.

IV   Investigation of Frequency
Weighted Cost Functionals

A simple open-loop unaugmented baseline system is analyzed. It is then augmented with a baseline controller whose penalty matrices are identity matrices. The performance and characteristics of the closed-loop baseline system with the baseline controller is compared to several of the frequency weighted controllers proposed by Gupta. The two types of controllers that are examined use frequency dependent state penalty matrices and frequency dependent control penalty matrices. The two controllers are examined independently to isolate the effect of the state or control penalty matrix on the performance index. The Bode frequency response and time response characteristics of each closed-loop system is analyzed and compared with the baseline controller closed-loop system.

Baseline System

The baseline model is a second order linear system with an open-loop natural frequency of $\omega_n = 1.0$ and damping of $\zeta = 0.2$. This simple lightly damped system is easy to analyze in terms of natural frequency and changes in damping. The corresponding characteristic equation for this system is the following:

$$s^2 + 0.4s + 1.0 = 0 \qquad (4\text{-}1)$$

The state equations for this system, expressed in phase variable control canonical form, are the following:

17

$$\frac{d}{dt} \begin{bmatrix} x(t) \\ \dot{x}(t) \end{bmatrix} = \begin{bmatrix} 0 & 1 \\ -1 & -0.4 \end{bmatrix} \begin{bmatrix} x(t) \\ \dot{x}(t) \end{bmatrix} + \begin{bmatrix} 0 \\ 1 \end{bmatrix} u(t) \qquad (4-2)$$

$$\underline{y}(t) = [1 \ 0] \ \underline{x}(t) \qquad (4-3)$$

The transfer function between the state $\underline{x}$ and the control $\underline{u}$ is calculated. Fig. 4-1 shows the Bode plot for the baseline system. The open-loop system has a high frequency slope of -40 dB/decade. The baseline system time response is shown in Fig. 4-2. The system has a peak time of t_p = 3.2 sec, peak overshoot of 53%, settling time t_s = 19.6 sec and final value of 1.00.

Baseline System with Baseline Controller

The baseline controller uses state and control penalty matrices that are identity matrices. That is:

$$\underline{Q} = \begin{bmatrix} 1 & 0 \\ 0 & 1 \end{bmatrix} \qquad \underline{R} = [1] \qquad (4-4)$$

and

$$J_{ss} = \int_{-\infty}^{\infty} \{ \underline{x}^{\star}(j\omega) \begin{bmatrix} 1 & 0 \\ 0 & 1 \end{bmatrix} \underline{x}(j\omega) + \mathbf{u}(j\omega)[1]u(j\omega) \} d\omega \quad (4-5)$$

While this simple case with identity $\underline{Q}$ and $\underline{R}$ matrices is not necessarily the best conventional controller, it serves as a good model to be compared with the controllers that use frequency weighted cost functionals. Table 4-1 shows the frequency response characteristics for the baseline controller.

18
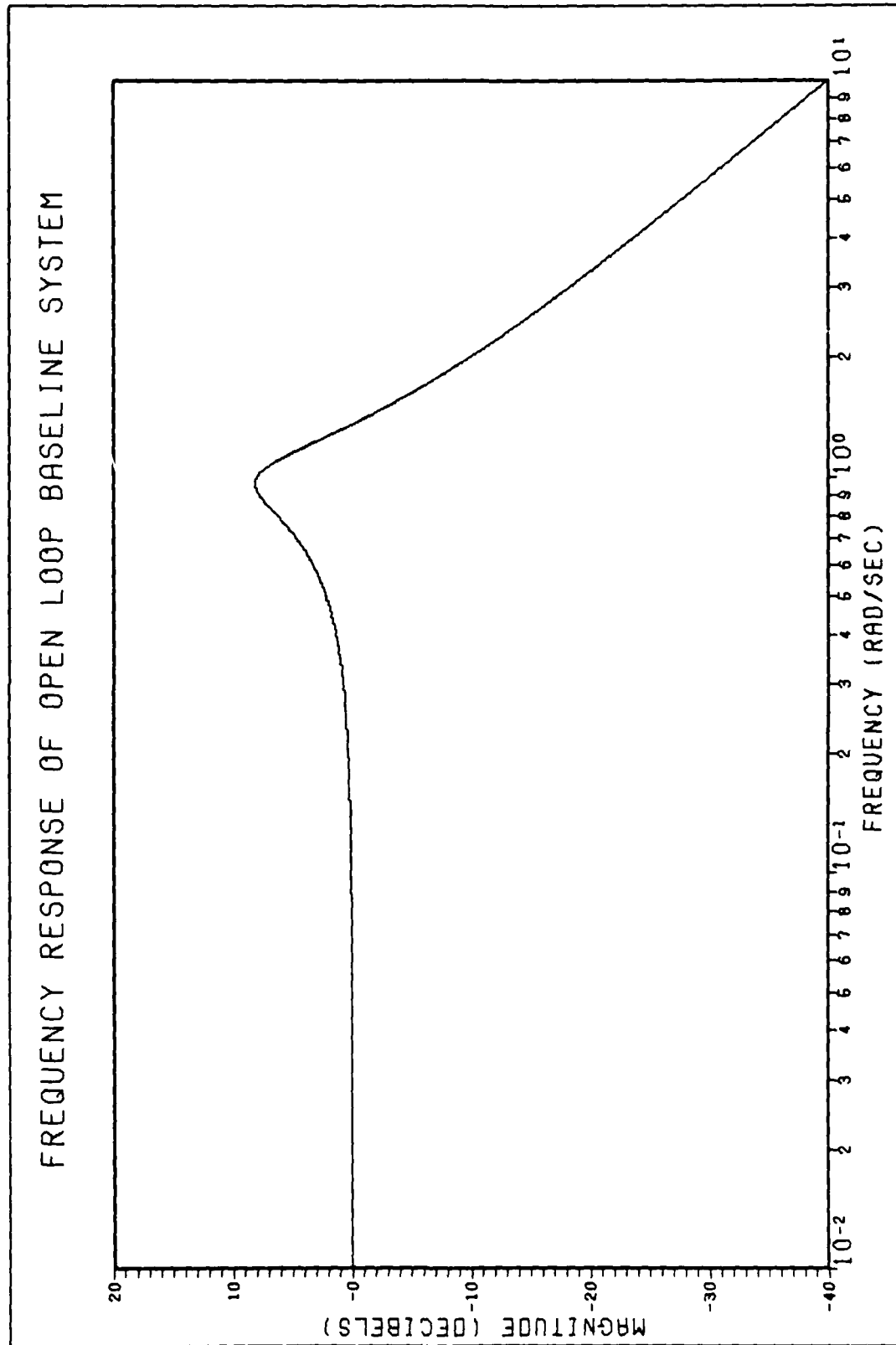
Fig. 4-1. Frequency Response of Open Loop Baseline System

TIME RESPONSE OF OPEN LOOP BASELINE SYSTEM
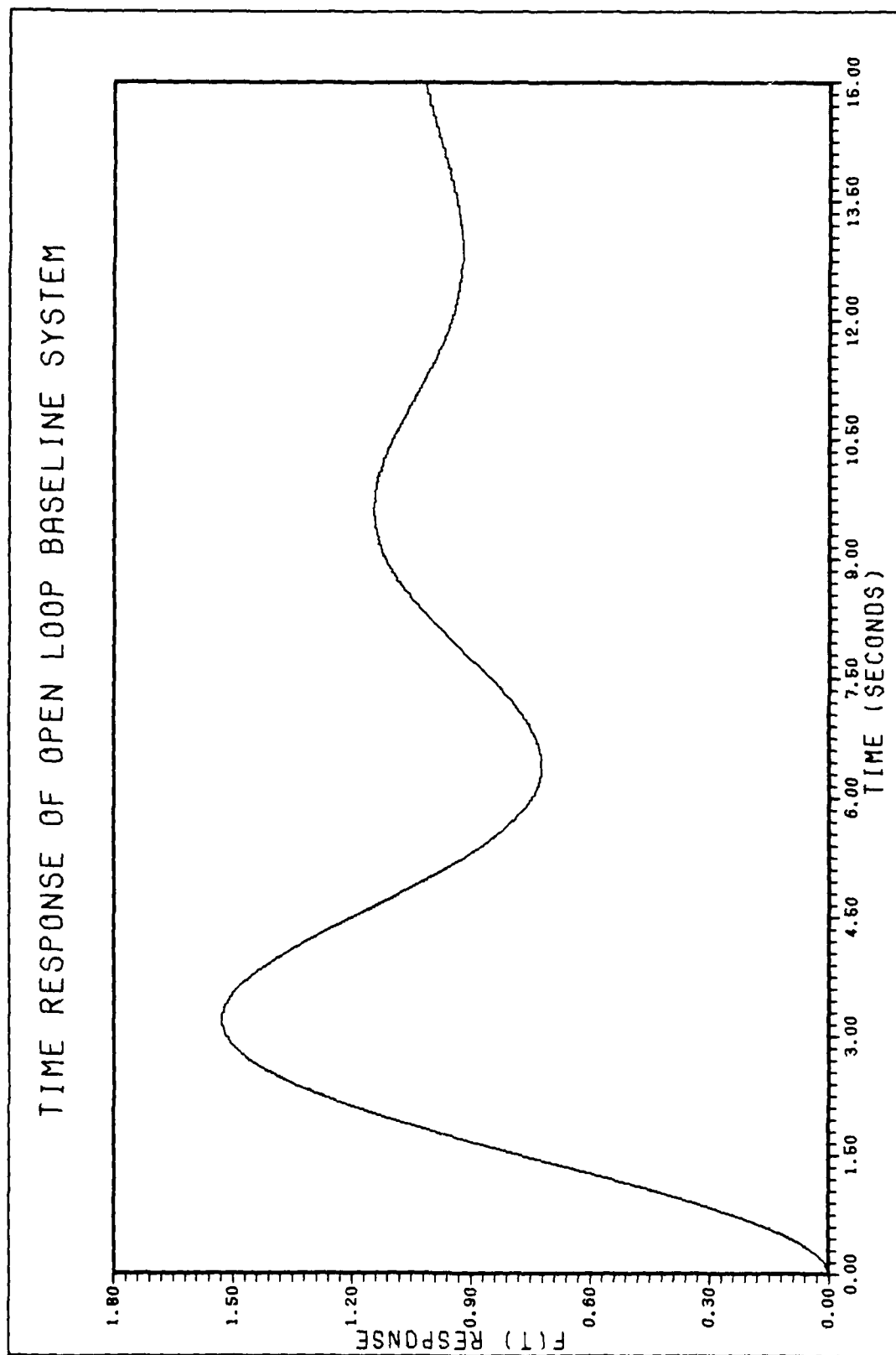
Fig. 4-2. Time Response of Open Loop Baseline System

20

Table 4-1. Characteristics of Baseline Controller

DC Gain	Closed-Loop Transfer Function		Natural Freq, ω_n	Damping Ratio ζ
	Gain	Poles		
0.708	1.00	$-0.705 \pm 0.958j$	1.19	0.593

This baseline controller system increased the damping to $\zeta = 0.593$, and had a natural frequency of $\omega_n = 1.19$. The Bode plot for this system is shown in Fig. 4-3. The dc gain is 0.708 and the high frequency rolloff slope is -40 dB/decade. Fig. 4-4 shows the time response of the baseline controller system. Using this system, the time response performance of the system was improved to the values shown in Table 4-2.

Table 4-2. Baseline Controller Time Response Characteristics

Rise Time (sec)	Peak Time (sec)	Settling Time (sec)	Peak Value	Final Value
1.54	3.28	4.99	0.777	0.707

Now the use of frequency weighted cost functionals is examined.

Case A

The first frequency weighted cost functional models a state penalty matrix that affects only the x_1 state, that is:
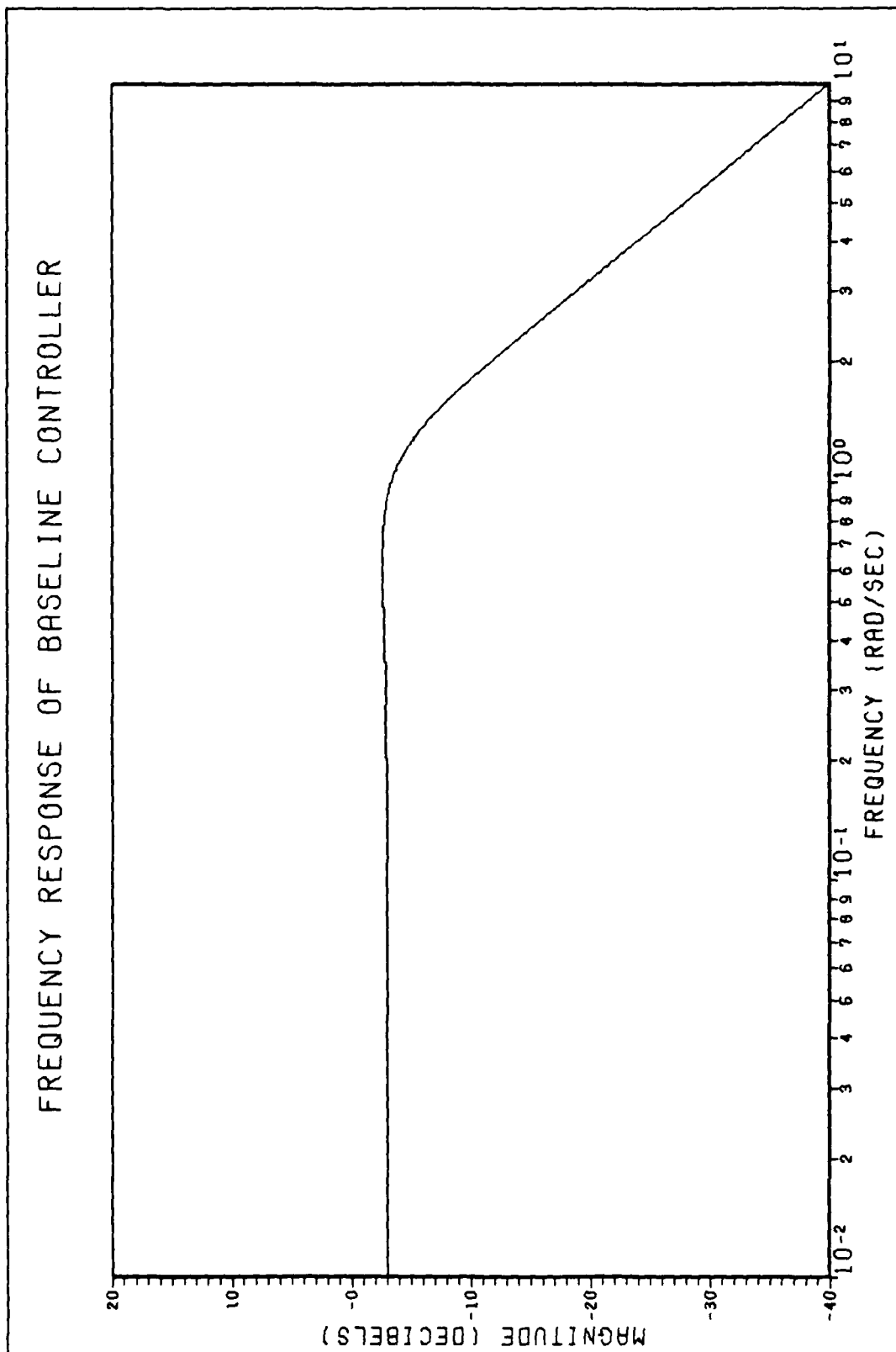
Fig. 4-3. Frequency Response of Baseline Controller

22

TIME RESPONSE OF BASELINE CONTROLLER
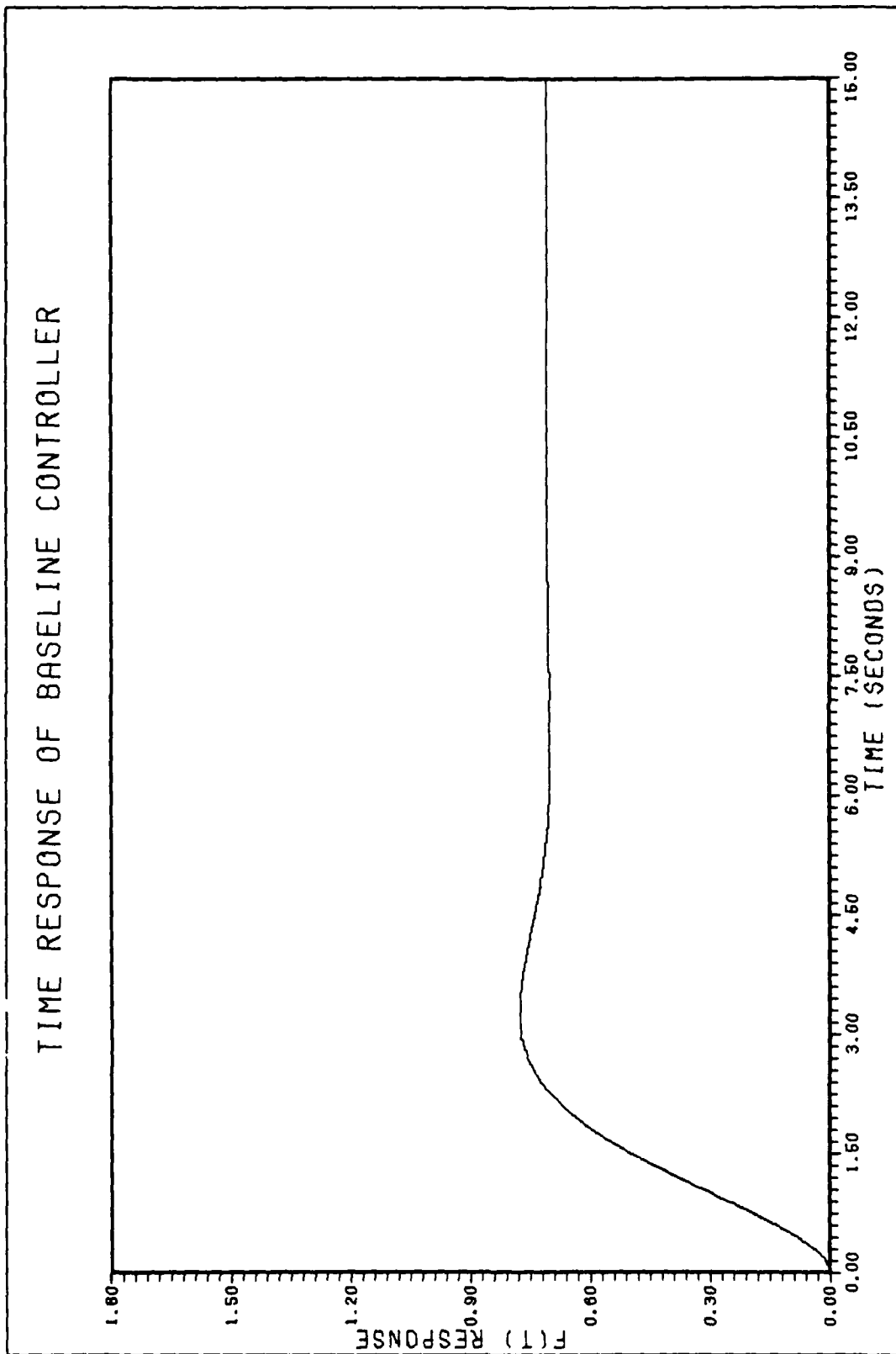
Fig. 4-4. Response of Baseline Controller

23

$$\underline{Q}(\omega) = \begin{bmatrix} \dfrac{1}{\omega^2 + a^2} & 0 \\ 0 & 1 \end{bmatrix} \tag{4-6}$$

and

$$J_{ss} = \int_{-\infty}^{\infty} \left\{ \underline{x}^*(j\omega) \begin{bmatrix} \dfrac{1}{\omega^2+a^2} & 0 \\ 0 & 1 \end{bmatrix} \underline{x}(j\omega) + u(j\omega) \ [1] \ u(j\omega) \right\} d\omega \tag{4-7}$$

Because this frequency weighting function has a numerator of smaller degree than the denominator, it is easy to form the realization for this system and implement the controller. Also, this $\underline{Q}$ matrix only affects the x_1 state and will be compared later to the effect of frequency weighting on both states. The $\underline{Q}$ matrix must be decomposed into the product $\underline{P}_1^*(j\omega) \ \underline{P}_1(j\omega)$ as described by Eq (2-15). This is done by the technique of spectral factorization (Ref 3: 507-8). The complex conjugate matrix factors of $\underline{Q}$ are the following:

$$\underline{P}_1(j\omega) = \begin{bmatrix} \dfrac{1}{j\omega+a} & 0 \\ 0 & 1 \end{bmatrix} ; \quad \underline{P}_1^*(j\omega) = \begin{bmatrix} \dfrac{1}{-j\omega+a} & 0 \\ 0 & 1 \end{bmatrix} \tag{4-8}$$

Therefore, the new variable $\underline{x}^1(j\omega)$ has been defined as follows:

$$\underline{x}^1(j\omega) = \begin{bmatrix} \dfrac{1}{j\omega+a} & 0 \\ 0 & 1 \end{bmatrix} \underline{x}(j\omega) \tag{4-9}$$

Recalling the augmented system equations

$$\underline{\dot{z}}_1(t) = \underline{A}_1 \underline{z}_1(t) + \underline{B}_1 \underline{x}(t) \tag{4-10}$$

24

$$\underline{x}^1(t) = \underline{C}_1 \underline{z}_1(t) + \underline{D}_1 \underline{x}(t) \qquad (4\text{-}11)$$

and if $\underline{x}^1(s) = \underline{H}(s)\underline{x}(s)$ according to Eqs (4-10) and (4-11)
then:

$$\underline{H}(s) = \underline{C}_1 (s\underline{I} - \underline{A}_1)^{-1} \underline{B}_1 + \underline{D}_1 \qquad (4\text{-}12)$$

However, instead of knowing the system matrices $\underline{A}_1$, $\underline{B}_1$, $\underline{C}_1$, and $\underline{D}_1$ and then solving for the transfer function matrix, $\underline{H}(s)$, the reverse is true. That is, the transfer function matrix between $\underline{x}_1(s)$ and $\underline{x}(s)$ has been defined by Eq (4-9) and the system matrices must be solved for. A realization (Ref 5:441-4) for this transfer function must be determined. Appendix B describes how to create a realization for a system. The following describes this particular realization:

$$\underline{P}_1(s) = \begin{bmatrix} \dfrac{1}{s+a} & 0 \\ 0 & 1 \end{bmatrix} \qquad (4\text{-}13)$$

$$\underline{z}_1(t) = [\underline{z}_1(t)] \qquad \underline{x}(t) = \begin{bmatrix} x_1(t) \\ x_2(t) \end{bmatrix} \qquad \underline{x}^1(t) = \begin{bmatrix} x_1^1 \\ x_2^1 \end{bmatrix} \qquad (4\text{-}14)$$

$$\underline{z}_1(t) = [-a]\,\underline{z}_1(t) + [1\ \ 0]\,\underline{x}(t) \qquad (4\text{-}15)$$

$$\underline{x}^1(t) = \begin{bmatrix} 1 \\ 0 \end{bmatrix} \underline{z}_1(t) + \begin{bmatrix} 0 & 0 \\ 0 & 1 \end{bmatrix} \underline{x}(t) \qquad (4\text{-}16)$$

where $\underline{A}_1 = [-a]$, $\underline{B}_1 = [1\ \ 0]$, $\underline{C}_1 = [1\ \ 0]^T$, and $D_1 = \begin{bmatrix} 0 & 0 \\ 0 & 1 \end{bmatrix}$ are the matrices described in the new system model, Eqs (4-10) and (4-11). Then we get the following:

25

$$\underline{H}(s) = \underline{C}_1 \ (s\underline{I} - \underline{A}_1)^{-1} \ \underline{B}_1 + \underline{D}_1 \qquad (4\text{-}17)$$

$$\underline{H}(s) = \begin{bmatrix} 1 & \frac{1}{s+a} \\ 0 & \frac{1}{s+a} \end{bmatrix} [1 \ \ 0] + \begin{bmatrix} 0 & 0 \\ 0 & 1 \end{bmatrix} \qquad (4\text{-}18)$$

$$\underline{H}(s) = \begin{bmatrix} \frac{1}{s+a} & 0 \\ 0 & 1 \end{bmatrix} \qquad (4\text{-}19)$$

Eq (4-19) checks with Eq (4-9) to show that

$$\underline{x}^1(s) = \begin{bmatrix} \dfrac{x_1(s)}{s+a} \\ x_2(s) \end{bmatrix} \qquad (4\text{-}20)$$

This new system model can be expressed in terms of both
the original and new systems by putting the model in the
form of Eq (2-27). Define the augmented state vector
$\tilde{\underline{x}}(t) = [\underline{x}(t) \ \underline{z}_1(t)]^T$.

$$\dot{\tilde{\underline{x}}}(t) = \tilde{\underline{A}} \ \tilde{\underline{x}}(t) + \tilde{\underline{B}} \ \tilde{\underline{u}}(t) \qquad (4\text{-}21)$$

$$\dot{\tilde{\underline{x}}}(t) = \begin{bmatrix} \underline{A} & \underline{0} \\ \underline{B}_1 & \underline{A}_1 \end{bmatrix} \tilde{\underline{x}}(t) + \begin{bmatrix} \underline{B} \\ \underline{0} \end{bmatrix} u(t) \qquad (4\text{-}22)$$

$$\tilde{\underline{y}}(t) = [\underline{C}_1 \ \ \underline{0}] \ \tilde{\underline{x}}(t) \qquad (4\text{-}23)$$

Therefore, the new system model is the following:

$$\dot{\tilde{\underline{x}}}(t) = \begin{bmatrix} 0 & 1 & \vdots & 0 \\ -1 & -0.4 & \vdots & 0 \\ 1 & 0 & \vdots & -a \end{bmatrix} \tilde{\underline{x}}(t) + \begin{bmatrix} 0 \\ 1 \\ 0 \end{bmatrix} \underline{u}(t) \qquad (4\text{-}24)$$

$$\dot{\tilde{\underline{y}}}(t) = [1 \ 0 \ 0] \ \tilde{\underline{x}}(t) \qquad (4\text{-}25)$$

The state penalty matrix, $\tilde{Q}$, is determined from the steady state performance Eq (2-31). Since only the state (and not the control) is being frequency shaped in this case, only the upper left quarter of the penalty matrix in Eq (2-31) is needed. Thus the penalty matrices are the following:

$$\tilde{Q} = \begin{bmatrix} \underline{D}_1^T \underline{D}_1 & \underline{D}_1^T \underline{C}_1 \\ \underline{C}_1^T \underline{D}_1 & \underline{C}_1^T \underline{C}_1 \end{bmatrix} = \begin{bmatrix} 0 & 0 & 0 \\ 0 & 1 & 0 \\ 0 & 0 & 1 \end{bmatrix} \qquad (4\text{-}26)$$

$$\underline{R} = [\underline{R}] = [1] \qquad (4\text{-}27)$$

The controllability matrix, $\tilde{M}_c$, for this realization is the following:

$$\tilde{\underline{M}}_c = [\tilde{\underline{B}}, \ \tilde{\underline{A}}\tilde{\underline{B}}, \ \tilde{\underline{A}}^2 \tilde{\underline{B}}] = \begin{bmatrix} 0 & 1 & -0.4 \\ 1 & -0.4 & -0.84 \\ 0 & 0 & 1 \end{bmatrix} \qquad (4\text{-}28)$$

Since $\tilde{\underline{M}}_c$ is of full rank, the augmented system is completely controllable.

Eq (4-24) represents the minimal realization of the system. Fortmann and Hitz describe a method to form the realization for a given transfer function (Ref 5:441-446). Their method is relatively easy, but it generally does not yield the minimal realization for a system. However, by knowing the non-minimal realization, it is easy to find the minimal realization. The non-minimal matrices are partitioned to rank $\tilde{\underline{M}}_c$ which yields the minimal realization. The non-minimal realization of the system is the following:

$$\dot{\underline{x}}(t) = \begin{bmatrix} 0 & 1 & \vdots & 0 & 0 \\ -1 & -0.4 & \vdots & 0 & 0 \\ 1 & 0 & \vdots & -a & 0 \\ 0 & 1 & \vdots & 0 & -a \end{bmatrix} \underline{\tilde{x}}(t) + \begin{bmatrix} 0 \\ 1 \\ 0 \\ 0 \end{bmatrix} u(t) \qquad (4\text{-}29)$$

$$\underline{\tilde{y}}(t) = [1 \ 0 \ 0 \ 0] \ \underline{\tilde{x}}(t) \qquad (4\text{-}30)$$

The difference between the above realization and the minimal realization is that the Riccati feedback gain matrix, $\underline{\tilde{K}}$, is not of full rank and the system is controllable but not completely observable.

The value of "a" ranged from 0.1 to 10.0 or 1/10 to 10 times the natural frequency of the open-loop baseline system. Table 4-3 shows the Riccati feedback gain, closed-loop transfer function between the state x, and input u, natural frequency, ω_n, damping, ζ, and dc gain for the various values of "a".

Bode plots for Case A are shown in Fig. 4-5. Each of the Case A augmented systems has an increased damping ratio. Compared with the baseline controller system, which has a damping ratio of $\zeta = 0.593$, the augmented systems with frequency shapings have dampings that range from 0.539 to 0.589. Like the baseline system, each of the augmented systems has a high frequency asymptote of -40 dB/decade. However, with a frequency weighting value, "a", at a larger value than the natural frequency, the magnitude response percent-overshoot, in the time domain, to a step input is much less. For a = 10 the frequency response is nearly flat until the break frequency where it drops off sharply at -40 dB/decade.

28

Table 4-3. Characteristics of System A

"a"	Riccati Feedback Gain, $\underline{K}$	Closed-Loop Transfer Function Zeros	Closed-Loop Transfer Function Poles	Natural Freq, ω_n	Damping ζ	DC Gain
10	[0.00494, 0.682, 0.000447]	−10.0	−0.541±0.844j, −10.0	1.002	0.539	1.0
5	[0.192, 0.695, 0.00317]	− 5.00	−0.547±0.849j, −5.00	1.01	0.542	0.977
0.5	[0.544, 1.10, 0.346]	− 0.50	0.575±0.993j, −0.849	1.15	0.501	0.447
0.1	[1.01, 1.38, 0.804]	− 0.10	0.564±1.01j, −0.753	1.16	0.488	0.10
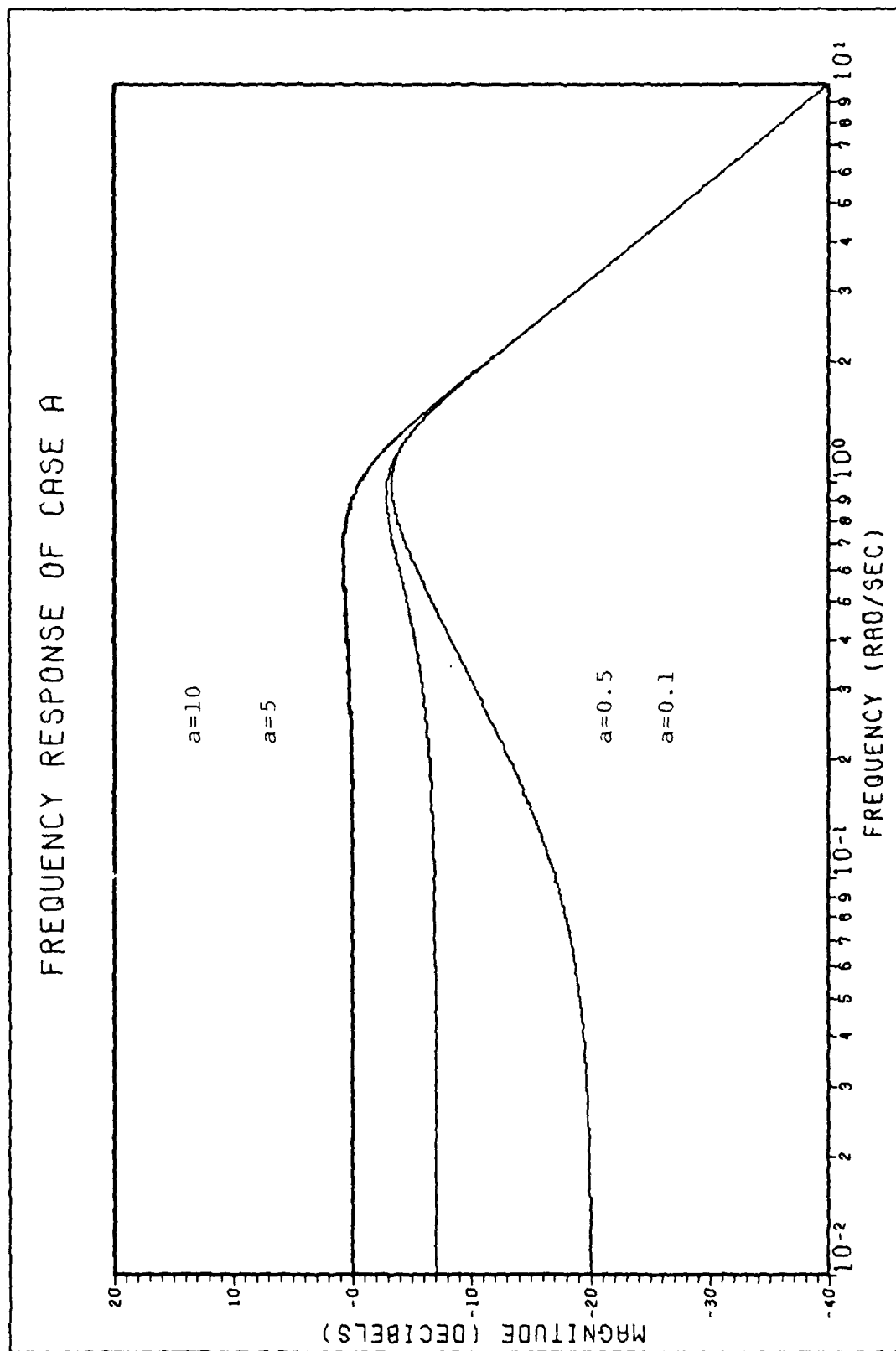
Fig. 4-5. Frequency Response of Case A

Fig. 4-6 shows the time responses for Case A. The time response for each of the augmented systems, with a unit step input, is much better than the original system. The systems with the larger values of "a" have increased damping over those with smaller values of "a" as shown in Table 4-4. The dc gains for the different cases vary greatly and result in the large difference in time response final values.

Table 4-4. Time Response Characteristics for System A

"a"	Rise Time (sec)	Peak Time (sec)	Settling Time (sec)	Peak Value	Final Value
10	1.71	3.72	5.79	1.13	0.995
5	1.70	3.70	5.75	1.11	0.981
0.5	0.989	2.65	7.25	0.630	0.447
0.1	0.347	2.11	10.2	0.442	0.0995
Baseline Controller	1.54	3.28	4.99	0.777	0.707

Table 4-4 shows that the closed-loop augmented system zeros are slightly smaller than the poles. In this regard, the controller acts like a lead filter, but over a very small frequency band. Therefore the effect of the zero-pole relationship is minimized. In general, the system performs best both in terms of frequency and time domain characteristics with values of "a" that are larger than the open-loop natural frequency. These results are not what I expected. For this frequency shaping of $1/(.^2+a^2)$,

31

TIME RESPONSE FOR CASE A
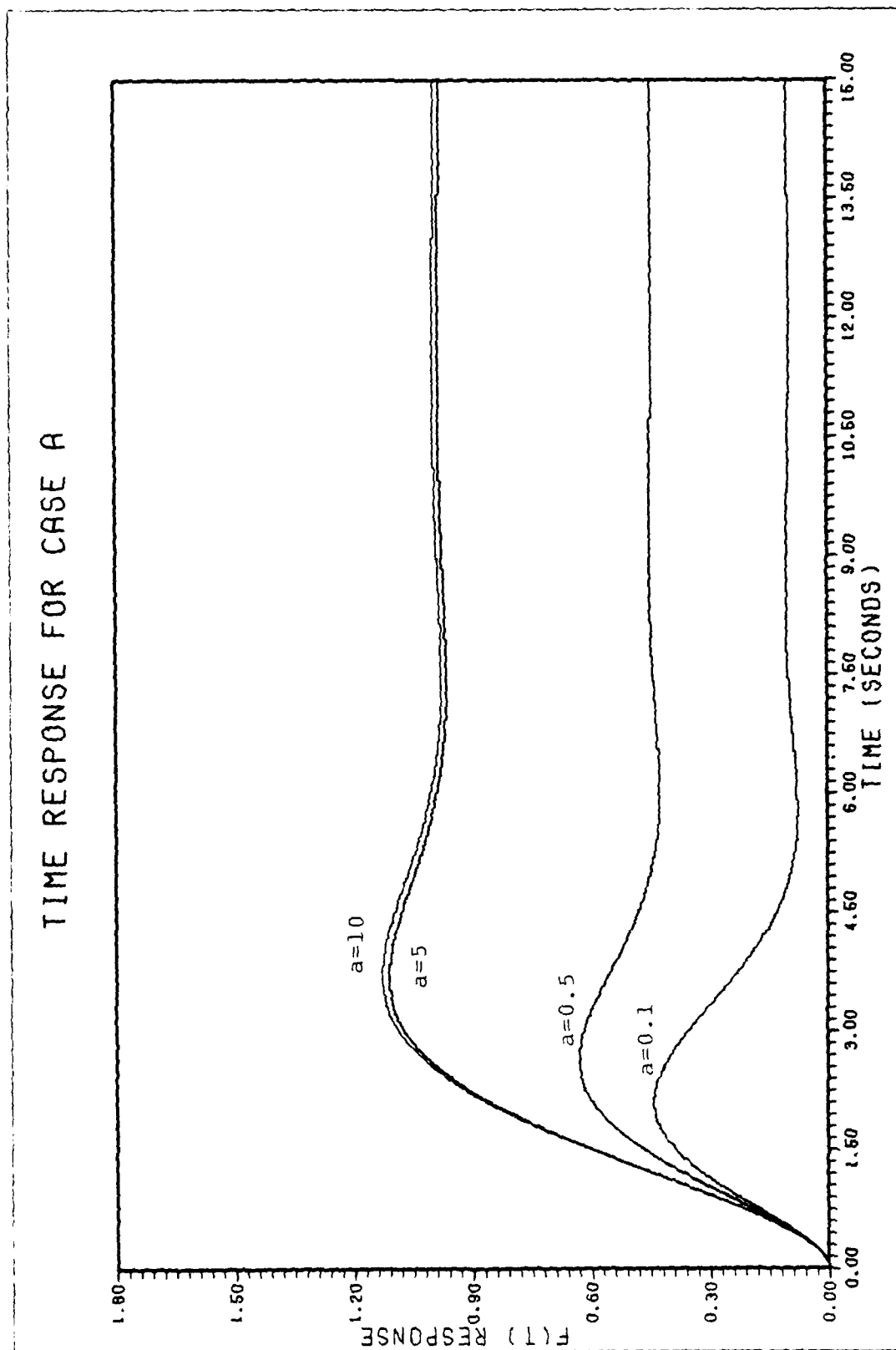
Fig. 4-6. Time Responses for Case A

I expected that as $\omega \to 0$ the low frequency weighting on x_1 would approach $1/a^2$. Similarly as $\omega \to \infty$ the ω^2 term would be the overwhelming term in the denominator and that the high frequency weighting would approach zero and the closed-loop high frequency response would be similar to the open-loop high frequency response. As Figs. 4-5 and 4-6 illustrate, all of the closed-loop responses have a larger damping ratio at all frequencies than the open-loop system.

Case B

The second frequency weighted cost functional models a penalty function that affects only the x_1 state, as before, but a numerator constant equal to the denominator constant, "a" is added as described below:

$$\underline{Q}(\omega) = \begin{bmatrix} \dfrac{a^2}{\omega^2+a^2} & 0 \\ 0 & 1 \end{bmatrix} \qquad (4-31)$$

This frequency shaping is identical to case A with the addition of the a^2 term in the numerator. I hoped that adding the numerator constant would cause the dc gain of the closed-loop systems to be the same for the different values of "a". Experience with classical frequency domain compensation techniques has shown that adding a numerator constant equal to the denominator constant normalizes the dc gain as desired. In the time domain this has the significance of normalizing the final response to a given input. I hoped that this $\underline{Q}(\omega)$ matrix would make it

33

easier to compare the performance of the closed-loop system with the different values of "a". Decomposing $\underline{Q}(\omega)$ into $\underline{P}_1^*(j\omega)$ and $\underline{P}_1(j\omega)$ we get the following:

$$\underline{P}_1(j\omega) = \begin{bmatrix} \dfrac{a}{j\omega+a} & 0 \\ 0 & 1 \end{bmatrix} \qquad \underline{P}_1^*(j\omega) = \begin{bmatrix} \dfrac{a}{-j\omega+a} & 0 \\ 0 & 1 \end{bmatrix} \qquad (4\text{-}32)$$

Recalling the augmented system equations:

$$\underline{\dot{z}}_1(t) = \underline{A}_1\underline{z}_1(t) + \underline{B}_1\underline{x}(t) \qquad (4\text{-}33)$$

$$\underline{x}^1(t) = \underline{C}_1\underline{z}_1(t) + \underline{D}_1\underline{x}(t) \qquad (4\text{-}34)$$

a realization for the system is defined to be the following:

$$\underline{\dot{z}}_1(t) = [-a]\,\underline{z}_1(t) + [a\ 0]\,\underline{x}(t) \qquad (4\text{-}35)$$

$$\underline{x}^1(t) = \begin{bmatrix} 1 \\ 0 \end{bmatrix}\underline{z}_1(t) + \begin{bmatrix} 0 & 0 \\ 0 & 1 \end{bmatrix}\underline{x}(t) \qquad (4\text{-}36)$$

Checking the transfer function between $\underline{x}^1(s)$ and $\underline{x}(s)$ described by Eq (4-32) we see that this is in fact a realization of the system.

$$\underline{P}_1(s) = \underline{C}_1\,(s\underline{I} - \underline{A}_1)^{-1}\,\underline{B}_1 + \underline{D}_1 \qquad (4\text{-}37)$$

$$= \begin{bmatrix} 1 & 1 \\ 0 & \dfrac{1}{s+a} \end{bmatrix} [a\ 0] + \begin{bmatrix} 0 & 0 \\ 0 & 1 \end{bmatrix} \qquad (4\text{-}38)$$

$$= \begin{bmatrix} \dfrac{a}{s+a} & 0 \\ 0 & 0 \end{bmatrix} + \begin{bmatrix} 0 & 0 \\ 0 & 1 \end{bmatrix} \qquad (4\text{-}39)$$

34

$$\underline{P}_1(s) = \begin{bmatrix} \dfrac{a}{s+a} & 0 \\ 0 & 1 \end{bmatrix} \qquad (4\text{-}40)$$

Defining the augmented system state variable $\tilde{\underline{x}} = [\underline{x} \ \underline{z}_1]^T$ the augmented system equations are the following:

$$\dot{\tilde{\underline{x}}}(t) = \tilde{\underline{A}} \ \tilde{\underline{x}}(t) + \tilde{\underline{B}} \ \underline{u}(t) \qquad (4\text{-}41)$$

$$\dot{\tilde{\underline{x}}}(t) = \begin{bmatrix} \underline{A} & 0 \\ \underline{B}_1 & \underline{A}_1 \end{bmatrix} \tilde{\underline{x}}(t) + \begin{bmatrix} \underline{B} \\ \underline{0} \end{bmatrix} \underline{u}(t) \qquad (4\text{-}42)$$

$$\dot{\tilde{\underline{x}}}(t) = \begin{bmatrix} 0 & 1 & 0 \\ -1 & -0.4 & 0 \\ \frac{-1}{a} & 0 & -a \end{bmatrix} \tilde{\underline{x}}(t) + \begin{bmatrix} 0 \\ 1 \\ 0 \end{bmatrix} \underline{u}(t) \qquad (4\text{-}43)$$

The augmented system penalty matrix, $\tilde{\underline{Q}}$ is determined again from the steady state performance Eq (2-31). Again we recall the following definition for the augmented state penalty matrix:

$$\tilde{\underline{Q}} = \begin{bmatrix} \underline{D}_1^T\underline{D}_1 & \underline{D}_1^T\underline{C}_1 \\ \underline{C}_1^T\underline{D}_1 & \underline{C}_1^T\underline{C}_1 \end{bmatrix} = \begin{bmatrix} 0 & 0 & 0 \\ 0 & 1 & 0 \\ 0 & 0 & 1 \end{bmatrix} \qquad (4\text{-}44)$$

The control penalty is the following:

$$\tilde{\underline{R}} = [\underline{R}] = [1] \qquad (4\text{-}45)$$

This realization is minimal. Table 4-5 describes the frequency response characteristics for Case B. Fig. 4-7 shows Bode plots for Case B with difference values of "a". The frequency response characteristics for the different

35

Table 4-5. Characteristics of System B

"a"	Riccati Feedback Gain, $\underline{K}$	Closed-Loop Transfer Function Zeros	Closed-Loop Transfer Function Poles	Natural Freq, ω_n	Damping Ratio, ζ	DC Gain
10	[0.410, 1.01, 0.00433]	-10.0	-0.703±0.959j -10.0	1.19	0.591	0.708
5	[0.399, 0.999, 0.0150]	- 5.00	-0.698±0.962j -5.004	1.19	0.587	0.708
1	[0.277, 0.910, 0.137]	- 1.00	-0.591±0.951j -1.13	1.12	0.528	0.708
0.5	[0.183, 0.836, 0.231]	- 0.500	-0.546±0.895j -0.644	1.05	0.521	0.708
0.1	[0.044, 0.717, 0.370]	- 0.100	-0.538±0.845j -0.141	1.002	0.537	0.708

36
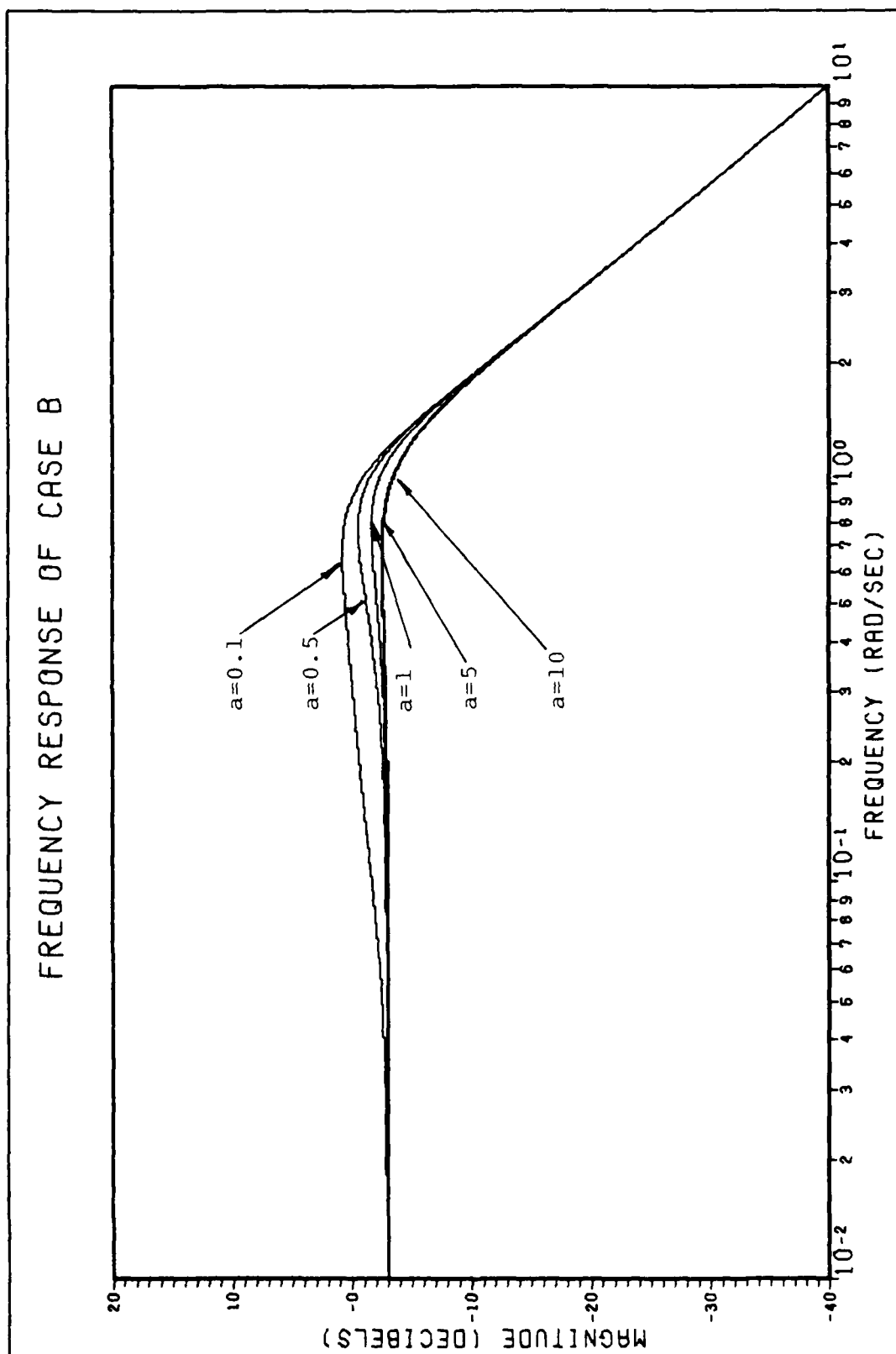
Fig. 4-7. Frequency Response of Case B

37

systems did not differ significantly. The natural frequency ranged from 1.19 to 1.002. In general, the damping ratio increased from $\zeta = 0.537$ for a = 0.1 to $\zeta = 0.591$ for a = 10. All of the systems had a very flat frequency response roll off. The controllers with large values of "a" have the smallest overshoot. The rolloff asymptote has a slope of -40 dB/decade. All of the systems have the same dc gain which is what was desired.

The time response characteristics of Case B, to a unity step input, are shown in Fig. 4-8. Adding the constant, "a", to the numerator makes all final values equal to 0.707. Table 4-6 shows that the time response characteristics are very similar for all values of "a". Using values of "a" that were less than the open-loop natural frequency resulted in greater overshoot, while larger "a" values had minimal overshoot. The frequency shapings for Case B performed somewhat similarly to

Table 4-6. Time Response Characteristics for System B

"a"	Rise Time (sec)	Peak Time (sec)	Settling Time (sec)	Peak Value	Final Value
10	1.54	3.27	4.98	0.778	0.707
5	1.53	3.26	4.98	0.779	0.707
1	1.42	3.17	7.00	0.824	0.707
0.5	1.33	3.19	7.63	0.885	0.705
0.1	1.21	3.49	Large	1.05	0.707

TIME RESPONSE FOR CASE B
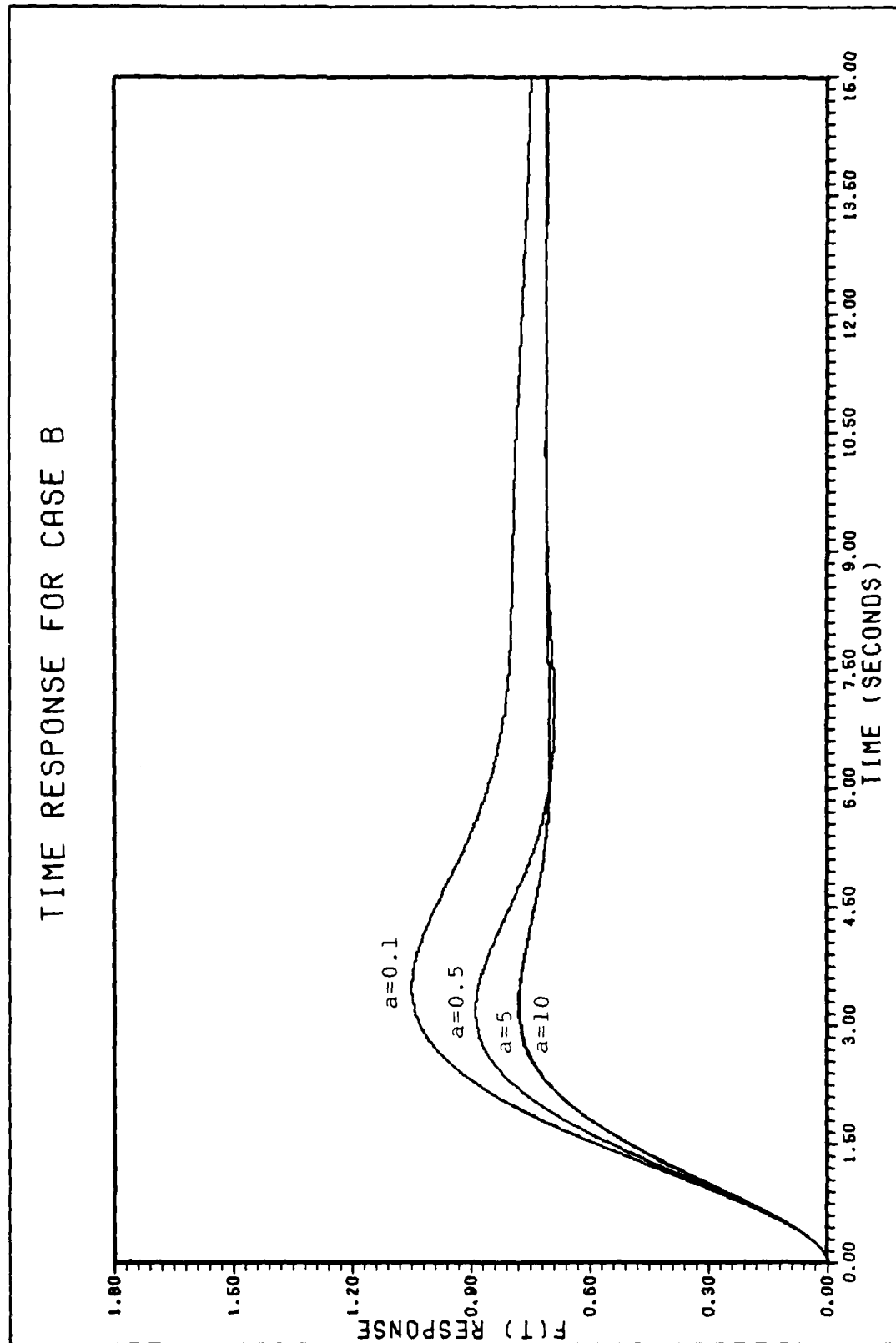
Fig. 4-8. Time Response for Case B

standard linear quadratic regulator designs. The frequency
shapings with larger values of "a" imposed a greater
penalty on state trajectory deviation than smaller values
of "a". In the neighborhood of the open-loop natural
frequency (e.g., from 0.1 to 10.0 rad/sec) the similarity
is closest. Using conventional linear quadratic methods,
for $\omega = 10$ the weighting for a = 10 is

$$\frac{a^2}{\omega^2 + a^2} = \frac{100}{100 + 100} = 0.5 \qquad (4-46)$$

and the weighting for a = 0.1 is

$$\frac{a^2}{\omega^2 + a^2} = \frac{0.01}{100 + 0.01} \cong 0.0001 \qquad (4-47)$$

At $\omega = 0.1$ the weighting for a = 10 is

$$\frac{a^2}{\omega^2 + a^2} = \frac{100}{0.01 + 100} \cong 1.0 \qquad (4-48)$$

and the weighting for a = 0.1 is

$$\frac{a^2}{\omega^2 + a^2} = \frac{0.01}{0.01 + 0.01} = 0.50 \qquad (4-49)$$

The smaller weightings behave more like the lightly damped
open-loop system and the larger weightings should result
in larger damping ratios. Qualitatively, the systems
using frequency weighted cost functionals behaved similarly
to systems with conventional cost functionals. Using larger

values of the frequency weighting results in larger damping ratios.

Case C

The third frequency weighted cost functional to be discussed is the same as Case B except that it affects both states, that is:

$$\underline{Q}(\omega) = \begin{bmatrix} \dfrac{a^2}{\omega^2+a^2} & 0 \\[3mm] 0 & \dfrac{a^2}{\omega^2+a^2} \end{bmatrix} \tag{4-50}$$

This case analyzes the effect of weighting both the x_1 and x_2 states instead of only x_1 in the previous case. The resulting change in the frequency and time response from the previous case is studied. Using spectral factorization, $\underline{Q}(\omega)$ is decomposed into the following values of $\underline{P}_1^*(j\omega)$ and $\underline{P}_1(j\omega)$:

$$\underline{P}_1(j\omega) = \begin{bmatrix} \dfrac{a}{j\omega+a} & 0 \\[3mm] 0 & \dfrac{a}{j\omega+a} \end{bmatrix} ; \quad \underline{P}_1^*(j\omega) = \begin{bmatrix} \dfrac{a}{-j\omega+a} & 0 \\[3mm] 0 & \dfrac{a}{-j\omega+a} \end{bmatrix} \tag{4-51}$$

The controller system state equations for the realization of this transfer function are the following:

$$\underline{\dot{z}}_1(t) = \begin{bmatrix} -a & 0 \\ 0 & -a \end{bmatrix} \underline{z}_1(t) + \begin{bmatrix} a & 0 \\ 0 & a \end{bmatrix} \underline{x}(t) \tag{4-52}$$

$$\underline{x}_1(t) = \begin{bmatrix} 1 & 1 \\ 0 & 0 \end{bmatrix} \underline{z}_1(t) + \begin{bmatrix} 0 & 0 \\ 0 & 0 \end{bmatrix} \underline{x}(t) \tag{4-53}$$

41

The verification that this system is, in fact, a realization of the transfer function between $\underline{x}^1(s)$ and $\underline{x}(s)$ is shown in Appendix C. The new system can be described by the following:

$$\dot{\underline{\tilde{x}}}(t) = \begin{bmatrix} 0 & 1 & | & 0 & 0 \\ -\frac{1}{a} & -0.4 & | & 0 & 0 \\ 0 & 0 & | & -a & 0 \\ 0 & a & | & 0 & -a \end{bmatrix} \underline{\tilde{x}}(t) + \begin{bmatrix} 0 \\ 1 \\ 0 \\ 0 \end{bmatrix} \underline{u}(t) \qquad (4\text{-}54)$$

The new penalty matrices $\tilde{Q}$ and $\tilde{R}$ are defined by Eq (2-31) to be the following:

$$\tilde{Q} = \begin{bmatrix} \underline{D}_1^T\underline{D}_1 & \underline{D}_1^T\underline{C}_1 \\ \underline{C}_1^T\underline{D}_1 & \underline{C}_1^T\underline{C}_1 \end{bmatrix} = \begin{bmatrix} 0 & 0 & 0 & 0 \\ 0 & 0 & 0 & 0 \\ 0 & 0 & 1 & 0 \\ 0 & 0 & 0 & 1 \end{bmatrix} \qquad \tilde{R} = [\underline{R}] = [1] \qquad (4\text{-}55)$$

This realization is minimal. Table 4-7 shows the frequency response characteristics for Case C. Values of the value "a", which are larger than the natural frequency have much higher damping ratios ($\zeta = 0.591$) than the original system. Unlike the previous cases, however, smaller values of "a" reduce the system damping ratio to nearly the same value ($\zeta = 0.210$) as the baseline system. This is because $\underline{Q}(\omega)$ approaches zero as "a" approaches zero which results in the augmented system responding more like the open-loop system. Fig. 4-9 shows the Bode plots for Case C. The Bode plots are significantly different because of the differences in damping ratios, discussed previously. Using a value of a = 10 caused the system to have a flat magnitude response with little overshoot. Conversely, the

42

Table 4-7. Characteristics of System C

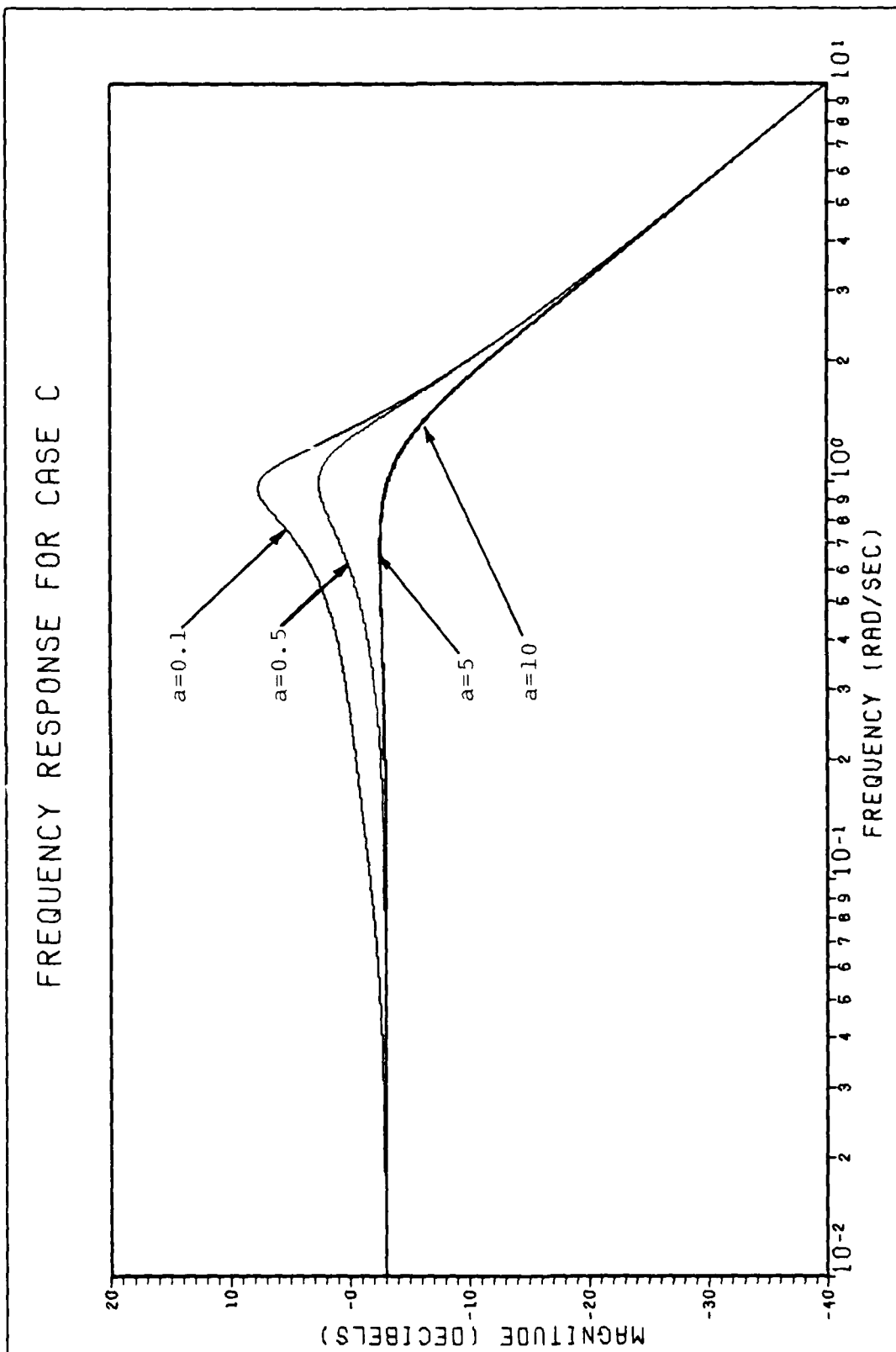| "a"	Riccati Feedback Gain, K	Closed-Loop Transfer Function		Natural Freq, ω_n	Damping Ratio, ζ	DC Gain
		Zeros	Poles			
10	[0.410, 0.959, 0.00434, 0.0434]	-10.0	$-0.704 \pm 0.962j$ -9.95	1.19	0.591	0.708
5	[0.399, 0.409, 0.0151, 0.0754]	- 5.00	$-0.701 \pm 0.975j$ -4.91	1.20	0.584	0.708
0.5	[0.159, 0.378, 0.255, 0.128]	- 0.50	$-0.346 \pm 1.04j$ -0.586	1.10	0.315	0.708
0.1	[0.0225, 0.0613, 0.392, 0.0392]	- 0.10	$-0.211 \pm 0.985j$	1.01	0.210	0.708

43

FREQUENCY RESPONSE FOR CASE C

Fig. 4-9. Frequency Response of Case C

44

systems with values of "a" smaller than the natural frequency have large magnitude overshoot at the break frequency. Table 4-7 shows that the natural frequencies are fairly constant for the different values of "a". The high frequency asymptote for all of the Case C systems is -40 dB/decade.

These results can be expected. By imposing frequency shaping on both states, the maximum value that $Q(\omega)$ can have is unity, so shapings with large values of "a" should be similar to the previous case which also has a maximum weighting approaching unity. However, for small values of "a", as "a" approaches zero, both state weightings approach zero. The biggest difference between this case and the previous case should be, and is, in systems involving smaller values of "a", which results in smaller damping ratios.

The time response characteristics for Case C are shown in Fig. 4-10. Table 4-8 shows that for larger values of "a", the systems have less overshoot with good time-to-peak-value properties. The time response characteristics for systems with small values of "a" have smaller damping ratios and are not much better than the open-loop response. Frequency weighting on both states has a much more varied effect on both frequency and time response characteristics than the previous cases. Changing the values of "a" causes very different responses, unlike Case B that uses frequency weighting on only one state.
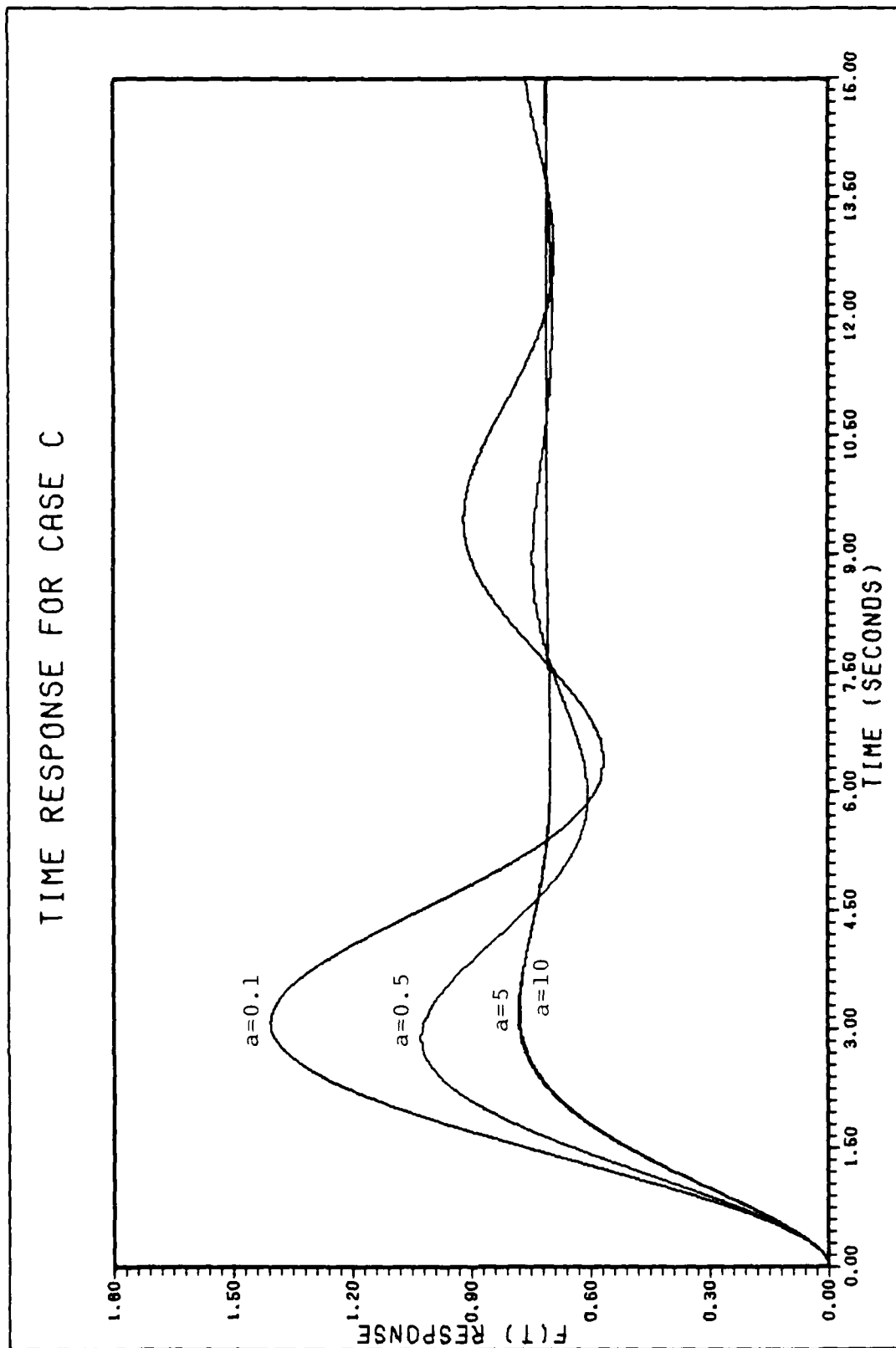
45

TIME RESPONSE FOR CASE C

F(T) RESPONSE

TIME (SECONDS)

a=0.1
a=0.5
a=5
a=10

Fig. 4-10. Time Responses for Case C

Table 4-3.   Time Response Characteristics for System C

"a"	Rise Time (sec)	Peak Time (sec)	Settling Time (sec)	Peak Value	Final Value
10	1.54	3.27	4.97	0.778	0.707
5	1.51	3.23	4.93	0.781	0.707
0.5	1.10	2.90	10.2	1.03	0.707
0.1	0.952	3.10	23.6	1.40	0.707

Case D

The fourth frequency weighted cost functional to be discussed uses both numerator and denominator weighting values on both state terms, that is:

$$\underline{Q}(\omega) = \begin{bmatrix} \dfrac{\omega^2+a^2}{\omega^2+b^2} & 0 \\ 0 & \dfrac{\omega^2+a^2}{\omega^2+b^2} \end{bmatrix} \tag{4-56}$$

Gupta suggests this improper weighting form because it provides a wide variety of ways to shape the response of the closed-loop system. $\underline{Q}(\omega)$ is factored into the terms $\underline{P}_1^*(j\omega)$ and $\underline{P}_1(j\omega)$ in the following manner:

$$\underline{P}_1(j\omega) = \begin{bmatrix} \dfrac{j\omega+a}{j\omega+b} & 0 \\ 0 & \dfrac{j\omega+a}{j\omega+b} \end{bmatrix} \quad \underline{P}_1^*(j\omega) = \begin{bmatrix} \dfrac{-j\omega+a}{-j\omega+b} & 0 \\ 0 & \dfrac{-j\omega+a}{-j\omega+b} \end{bmatrix} \tag{4-57}$$

The augmented system equations are put into the form of Eqs (2-23) and (2-24) and the modified system equations become the following:

47

$$\dot{\underline{z}}_1(t) = \begin{bmatrix} -b & 0 \\ 0 & -b \end{bmatrix} \underline{z}_1(t) + \begin{bmatrix} 1 & 0 \\ 0 & 1 \end{bmatrix} \underline{x}(t) \qquad (4\text{-}58)$$

$$\underline{x}^1(t) = \begin{bmatrix} a-b & 0 \\ 0 & a-b \end{bmatrix} \underline{z}_1(t) + \begin{bmatrix} 1 & 0 \\ 0 & 1 \end{bmatrix} \underline{x}(t) \qquad (4\text{-}59)$$

Appendix D illustrates how to form a realization for this system. The augmented system can be described by the following state equation:

$$\dot{\underline{x}}(t) = \begin{bmatrix} 0 & 1 & 0 & 0 \\ -1 & -0.4 & 0 & 0 \\ 1 & 0 & -b & 0 \\ 0 & 1 & 0 & -b \end{bmatrix} \tilde{\underline{x}}(t) + \begin{bmatrix} 0 \\ 1 \\ 0 \\ 0 \end{bmatrix} \underline{u}(t) \qquad (4\text{-}60)$$

The augmented state penalty matrix is defined by the $\underline{C}_1$ and $\underline{D}_1$ matrices in Eq (4-59) to be the following:

$$\tilde{\underline{Q}} = \begin{bmatrix} \underline{D}_1^T \underline{D}_1 & \underline{D}_1^T \underline{C}_1 \\ \underline{C}_1^T \underline{D}_1 & \underline{C}_1^T \underline{C}_1 \end{bmatrix} = \begin{bmatrix} 1 & 0 & (a-b) & 0 \\ 0 & 1 & 0 & (a-b) \\ (a-b) & 0 & (a-b)^2 & 0 \\ 0 & (a-b) & 0 & (a-b)^2 \end{bmatrix} \qquad (4\text{-}61)$$

This realization is minimal. Table 4-9 shows the characteristics for system D. Using both numerator and denominator weightings provides a wider variety of ways to shape the baseline system. Using a parameter value of a = 10, larger than the open-loop natural frequency, and a value of b = 0.1, smaller than the natural frequency, the damping ratio is increased significantly to ζ = 0.657 and the new natural frequency increases threefold to 3.19. Using values of a = 1.0 and b = 2.0, the damping ratio is increased moderately to ζ = 0.4 and the natural frequency,

Table 4-9. Characteristics of System D

"a", "b"	Riccati Feedback Gain, $\underline{K}$	Closed-Loop Transfer Function Zeros	Poles	Natural Freq, ω_n	Damping Ratio, ζ	DC Gain
a = 10 b = 0.1	[12.0, 4.79, 8.70, 0.870]	-0.100	-2.16±2.35j -0.982	3.19	0.675	0.01
a = 2 b = 1	[0.944, 1.501, 0.292, 0.292]	-1.00	-0.953±1.15j -1.00	1.50	0.637	0.447
a = 2 b = 0.5	[1.60, 1.86, 0.760, 0.380]	-0.50	-0.974±1.26j -0.816	1.59	0.613	0.237
a = 2 b = 0.1	[2.68, 2.22, 1.63, 0.163]	-0.10	-0.975±1.29j -0.767	1.62	0.604	0.050
a = 1 b = 2	[0.171, 0.639, -0.105, -0.211]	-2.00	-0.470±0.919j -2.10	1.032	0.455	0.891
a = 0.5 b = 2	[-0.1001, 0.496, -0.140, -0.279]	-2.00	-0.387±0.907j -2.12	0.986	0.393	0.966
a = 0.1 b = 10	[0.00479, 0.0707, -0.0474, -0.474]	-10.0	-0.211±0.975j -10.1	0.998	0.212	1.00
a = 0.1 b = 2	[0.0772, 0.4401, -0.152, -0.304]	-2.00	-0.167±0.958j -2.11	0.972	0.172	1.00

ω_n = 1.032 is almost the same as the baseline system. For the case of a = 0.1 and b = 2, the least damping, ζ = 0.172 occurs. This damping is significantly less than the baseline system.

Intermediate values of "a" and "b" give widely different damping ratios and natural frequencies. Fig. 4-11 shows Bode plots of selected values of "a" and "b". The system with a = 2, b = 1 shows a nearly flat magnitude response until the break frequency where the slope drops off at -40 dB/decade. All of the high frequency asymptotes drop off at -40 dB/decade. This particular case behaves similarly to a lead filter in terms of the pole-zero location in that the closed-loop system zero is less negative than the dominant pole, and there is a large increase in ω_n which reduces the settling time. The closed-loop transfer function has a dc gain which is less than unity. To normalize each of the Case D systems, so that each system had the same dc gain, the frequency weightings could have been multiplied by a constant equal to b/a. Therefore, as seen in Fig. 4-11, the low frequency magnitude could be increased by multiplying by the additional gain.

Fig. 4-11 and Table 4-9 show varying degrees of the lead filter effect for different values of "a" and "b". However, as "a" is held constant and "b" is decreased, the damping ratio decreases. Fig. 4-12 shows the time response for selected Case D systems. Table 4-10 shows
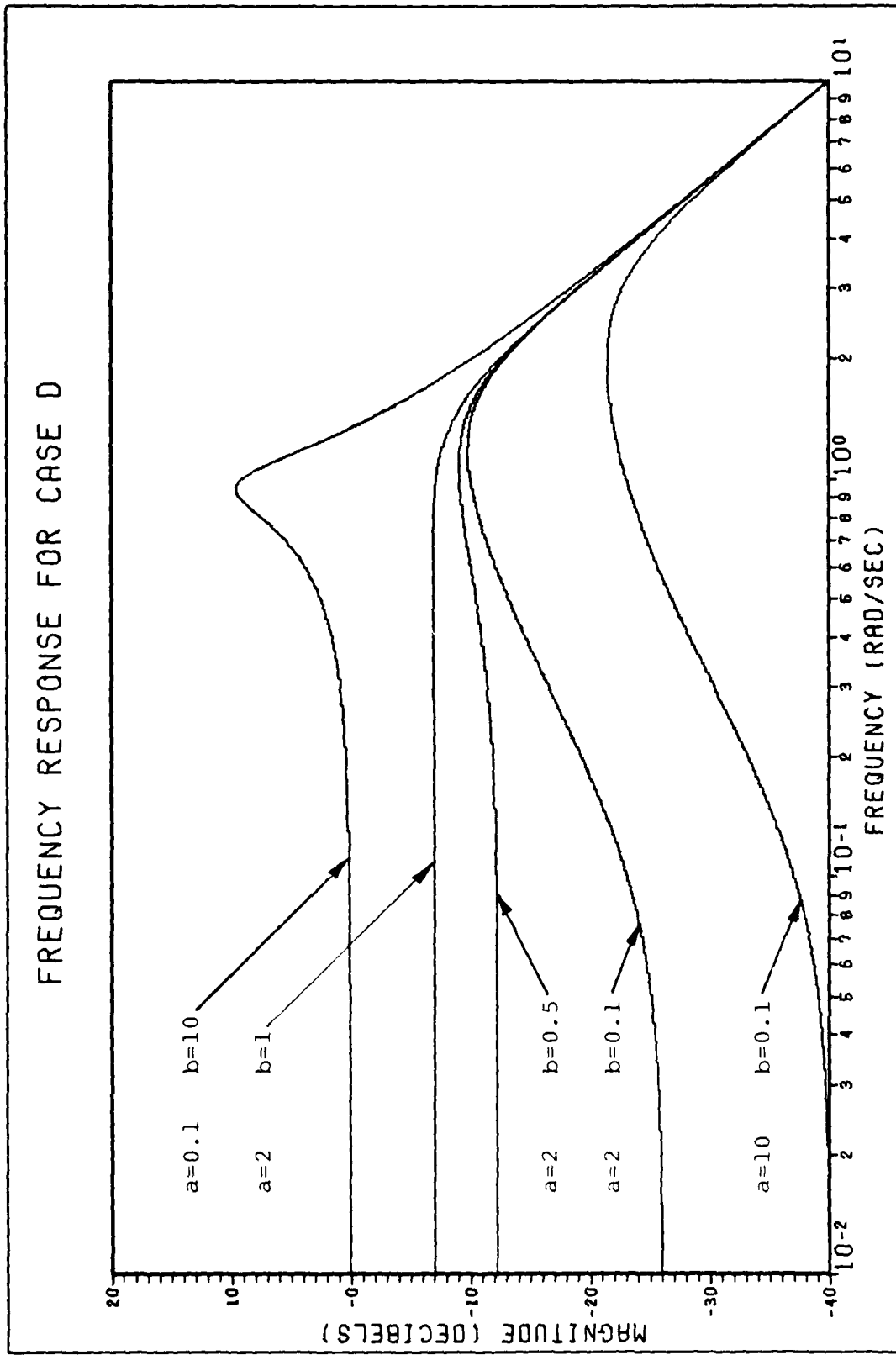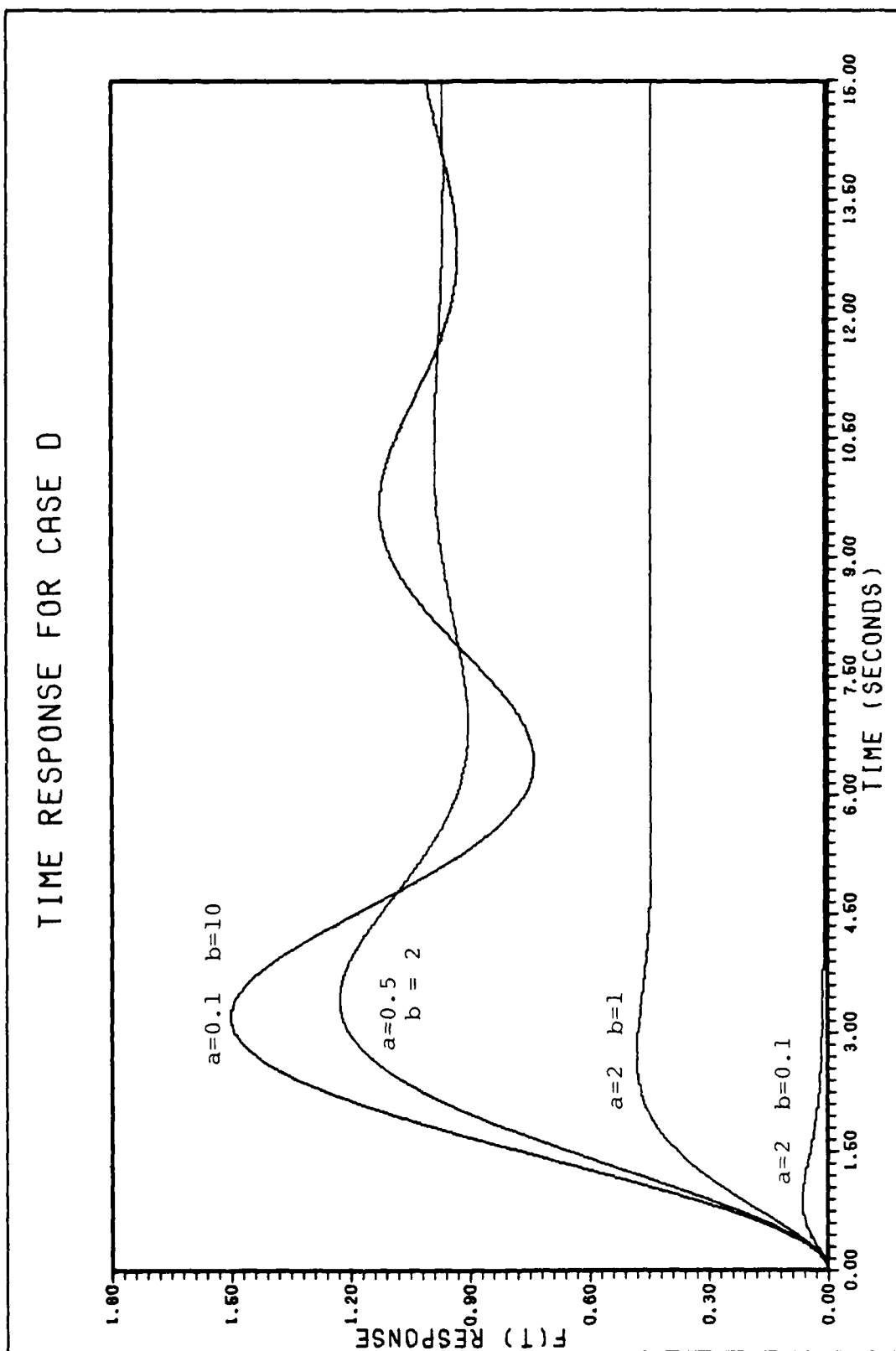
50

FREQUENCY RESPONSE FOR CASE D

a=0.1 b=10

a=2 b=1

a=2 b=0.5

a=2 b=0.1

a=10 b=0.1

MAGNITUDE (DECIBELS)

FREQUENCY (RAD/SEC)

Fig. 4-11. Frequency Response of Case D

51

Fig. 4-12. Time Responses for Case D

Table 4-10. Time Response Characteristics for System D

a=	b=	Rise Time (sec)	Peak Time (sec)	Settling Time (sec)	Peak Value	Final Value
10	0.1	0.107	0.987	Large	0.065	0.01
2	1.0	1.30	2.73	4.01	0.481	0.447
2	0.5	0.775	2.05	4.32	0.327	0.242
2	0.1	0.248	1.61	8.26	0.232	0.05
1	2	1.49	3.39	8.05	1.07	0.894
0.5	2	1.45	3.43	8.50	1.23	0.970
0.1	10	1.22	3.22	17.1	1.51	1.00
0.1	2	1.19	3.26	23.4	1.59	1.00

the time response characteristics for Case D. The systems
with smaller values of "a" and larger values of "b", (a =
0.1, b = 10), have smaller damping ratios, ζ = 0.212, and
greater values for overshoot and settling time. The system
with a = 2, b = 0.1, on the other hand, has a much smaller
time response.

In general, Case D systems provide much more flex-
ibility in designing system response than the previous
three cases. Wide ranges of frequency and time response
characteristics can be achieved depending on the choice of
"a" and "b". Let us assume that a design objective is to
reject disturbances. The system can be modeled by the
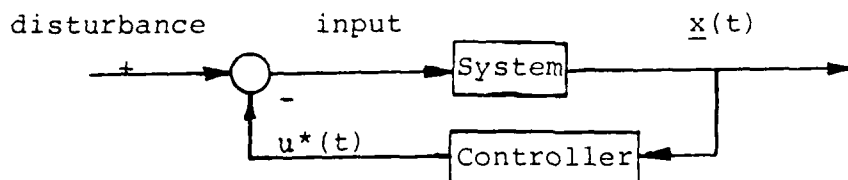following block diagram:

disturbance   input $\underline{x}(t)$

+ → ⊖ → System ——————————→
         −
      $u^*(t)$ ← Controller ←——

53

Fig. 4-11 shows Bode plots for the frequency response between the state, x_1, and commanded control u_c. If u_c is assumed to be some disturbance instead, then the Bode plots can be interpreted as the frequency response of the transfer function between x_1 and some distrubance. Comparing the various Bode plots in terms of distrubance rejection, one characteristic that is desirable is small dc gains. This indicates that reduced magnitude response occurs at lower frequencies. If the goal is to reject low frequency disturbances, then the more negative the low frequency response magnitude in decibels, the better. From Fig. 4-11, the system with $a = 2$, $b = 1$ is better at rejecting zero-mean white Gaussian noise. The system with $a = 10$, $b = 0.1$ is much better than the baseline controller closed-loop system at rejecting low frequency noise because the low frequency penalty on state x_1 is much higher. Small "a" values and large "b" values create a lightly damped, slower responding system, while large "a" values and small "b" values create a highly damped, faster system.

Case E

Unlike the previous cases, this case examines frequency weighting on the control instead of the state. One model proposed by Gupta (Ref 7:5) is the following:

$$R(j\omega) = \left[\frac{j\omega + a}{a} \right] \tag{4-62}$$

With the previous state weightings it was not possible to use frequency shapings with a numerator of greater degree

54

than the denominator. However, by including the control
in the state vector it is possible to realize the control
weighting given by Eq (4-62). The purpose is to see if
this type of frequency shaping on the control can change
the damping ratio and natural frequency of the closed-loop
system. Recalling Eqs (2-25) and (2-26), the augmented
system can be described by the following:

$$\dot{\underline{z}}_2(t) = \underline{A}_2\underline{z}_2(t) + \underline{B}_2\underline{u}(t) \tag{4-63}$$

$$\underline{u}^1(t) = \underline{C}_2\underline{z}_2(t) + \underline{D}_2\underline{u}(t) \tag{4-64}$$

where the new control variable, $u^1(t)$, is a linear combina-
tion of the commanded control, $u(t)$, and some frequency
weighted function of $u(t)$. That is, the new control
variable is defined to be the following:

$$u^1(s) = \left[\frac{s+a}{a}\right] u(s) \tag{4-65}$$

or equivalently:

$$au^1(t) = \dot{u}(t) + au(t) \tag{4-66}$$

$$\dot{u}(t) = au(t) - au^1(t) \tag{4-67}$$

This case of frequency weighting is the same as including
control (actuator) dynamics into the state equation. This
system is easily modeled and a realization is easy to find.
The augmented system, with the new control variable u^1 is
defined by the following state equation:

$$\frac{d}{dt} \begin{bmatrix} x(t) \\ \dot{x}(t) \\ u(t) \end{bmatrix} = \begin{bmatrix} \underline{A} & \vdots & \underline{B} \\ \underline{0} & \vdots & -a \end{bmatrix} \begin{bmatrix} x(t) \\ \dot{x}(t) \\ u(t) \end{bmatrix} + \begin{bmatrix} 0 \\ 0 \\ +a \end{bmatrix} u^1(t) \qquad (4\text{-}68)$$

or, for this specific case:

$$\frac{d}{dt} \begin{bmatrix} x(t) \\ \dot{x}(t) \\ u(t) \end{bmatrix} = \begin{bmatrix} 0 & 1 & \vdots & 0 \\ -1 & -0.4 & \vdots & 1 \\ 0 & 0 & \vdots & -a \end{bmatrix} \begin{bmatrix} x(t) \\ \dot{x}(t) \\ u(t) \end{bmatrix} + \begin{bmatrix} 0 \\ 0 \\ a \end{bmatrix} u^1(t) \qquad (4\text{-}69)$$

where $\underline{A}_2 = [-a]$ and $\underline{B}_2 = [a]$. In order to analyze the
frequency response of this case, the transfer function
between the commanded input $u(S)$ and the state $\underline{x}(S)$ must
be determined. This cannot be done outright from Eq (4-69)
because of the use of the new control variable u^1. The
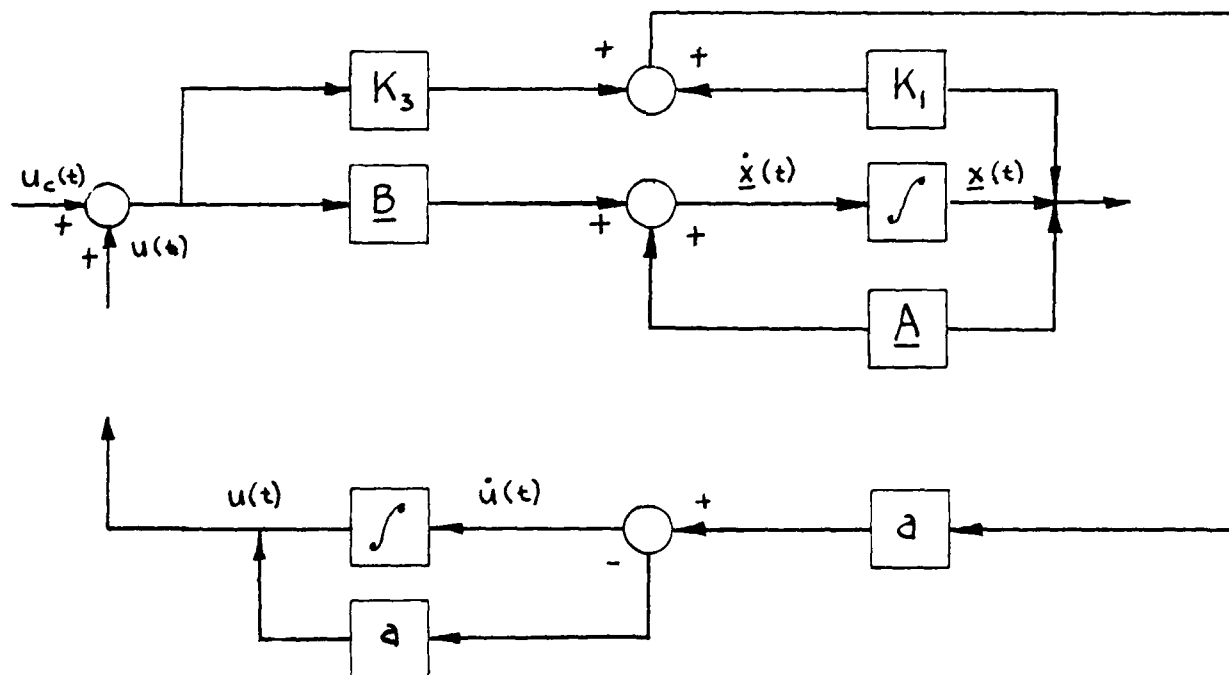entire system block diagram is shown in Fig. 4-13.

Fig. 4-13. Block Diagram of Case E

The loop must be closed on $\underline{u}(s)$ to calculate the transfer function between the state $\underline{x}(s)$ and the commanded input $\underline{u}_c(s)$. Appendix A shows that the transfer function matrix is the following:

$$\underline{H}(s) = \begin{bmatrix} \dfrac{(s+a - aK_3)}{s[(s+0.4)(s+a - aK_3) - aK_2] + (s+a - aK_3 - aK_1)} \\ \dfrac{-(s+a - aK_3)}{[(s+0.4)(s+a - aK_3) - aK_2] + (s+a - aK_3 - aK_1)} \end{bmatrix}$$

(4-70)

The identity matrix will be used for the state and control penalty matrices, that is:

$$\underset{\sim}{Q} = \begin{bmatrix} 1 & 0 & 0 \\ 0 & 1 & 0 \\ 0 & 0 & 1 \end{bmatrix} \qquad \underset{\sim}{R} = [1] \qquad (4-71)$$

Table 4-11 shows the frequency response characteristics for Case E. Large values of "a" (a = 10) result in larger values of the damping ratio, $\zeta = 0.208$ for a = 0.1. Bode plots for this case are shown in Fig. 4-14. Each system has very similar, flat low frequency response characteristics. All of the systems have improved magnitude overshoot properties compared with the open-loop baseline system. All Case E systems had larger overshoot than the closed-loop baseline controller. This is because the baseline weightings are unity while the frequency shaped weightings can only approach unity as "a" gets very large. The a = 10 system has the least overshoot of all. All Case E

Table 4-11. Characteristics of System E

| "a"	Riccati Feedback Gain, $\underline{K}$	Closed-Loop Gain	Transfer Function Poles	Natural Freq, ω_n	Damping Ratio, ζ	DC Gain
10	[0.254, 0.917, 0.478]	10.0	-0.526±0.974j, -14.1	1.11	0.475	0.575
2	[0.0431, 0.853, 0.689]	2.00	-0.509±0.998j, -2.76	1.12	0.455	0.575
1	[-0.132, 0.737, 0.864]	1.00	-0.445±1.03j, -1.38	1.12	0.396	0.575
0.5	[-0.290, -0.522, 1.02]	0.500	-0.335±1.03j, -0.741	1.08	0.310	0.575
0.1	[-0.194, 0.0854, 0.926]	0.100	-0.217±1.02j, -0.158	1.05	0.208	0.575

FREQUENCY RESPONSE FOR CASE E
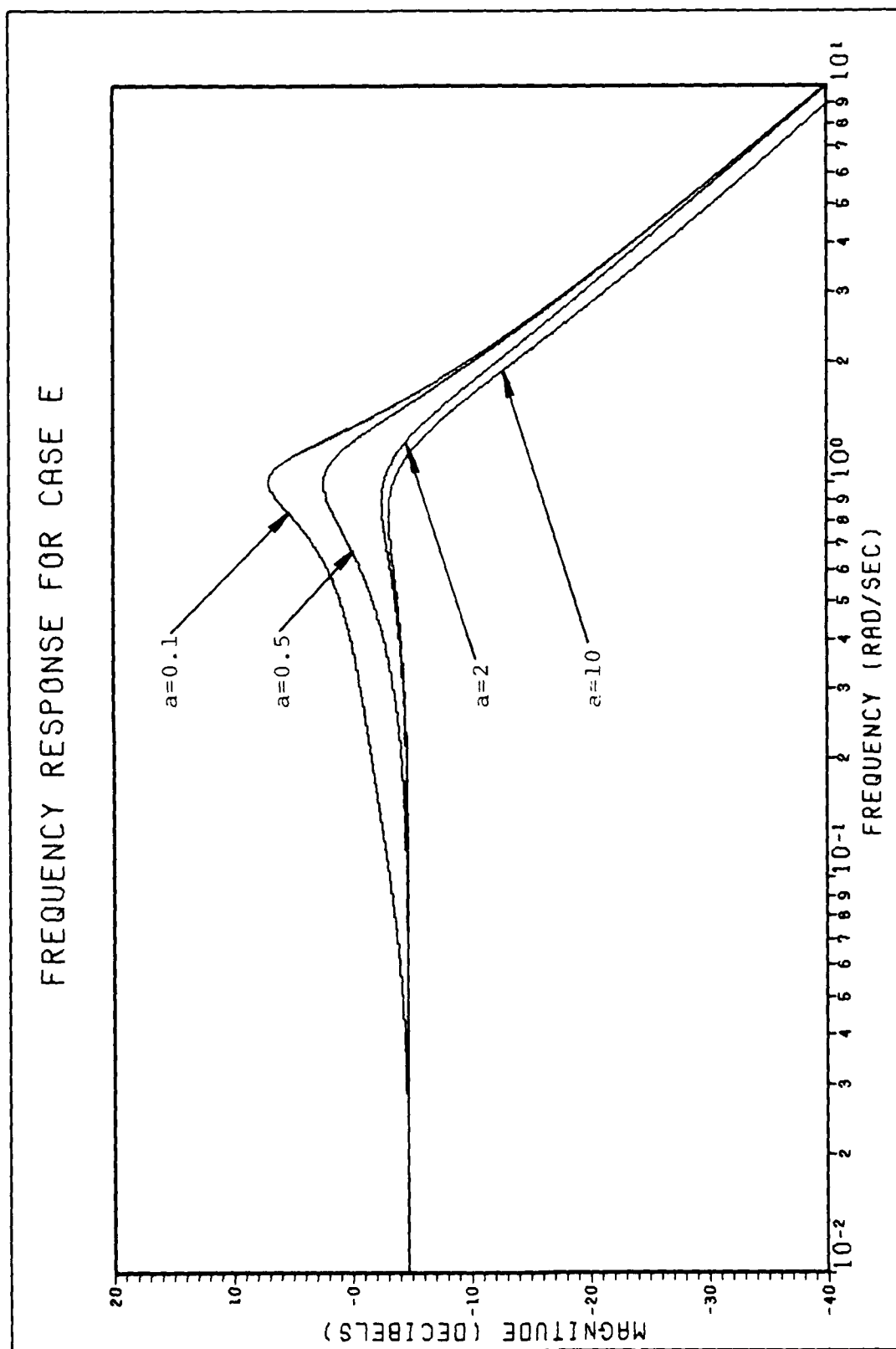
Fig. 4-14. Frequency Response of Case E

59

systems have a high frequency asymptote slope of -40 dB/ decade.

The time responses of Case E systems are shown in Fig. 4-15. Time response characteristics are shown in Table 4-12. The system with a = 0.1 has the largest peak value (1.27) and longest settling time (22.9 sec). The fastest system with the least overshoot has a parameter of a = 10 with a settling time of 7.42 sec and a peak value of 0.684.

Table 4-12. Time Response Characteristics for System E

"a"	Rise Time (sec)	Peak Time (sec)	Settling Time (sec)	Peak Value	Final Value
10	1.43	3.19	7.42	0.684	0.577
2	1.28	2.97	7.33	0.705	0.577
1	1.12	2.79	9.32	0.772	0.577
0.5	0.978	2.79	12.6	0.921	0.577
0.1	0.843	2.95	22.9	1.27	0.577

This method of frequency shaping can be useful in including control dynamics in a system. In terms of other systems, Case E qualitatively responds most like Case C which had the reciprocal frequency weighting on both states.

Case F

The frequency weighted cost functional for this case attempts to drive the state penalty weighting to a very large value at some specified frequency. Gupta suggests
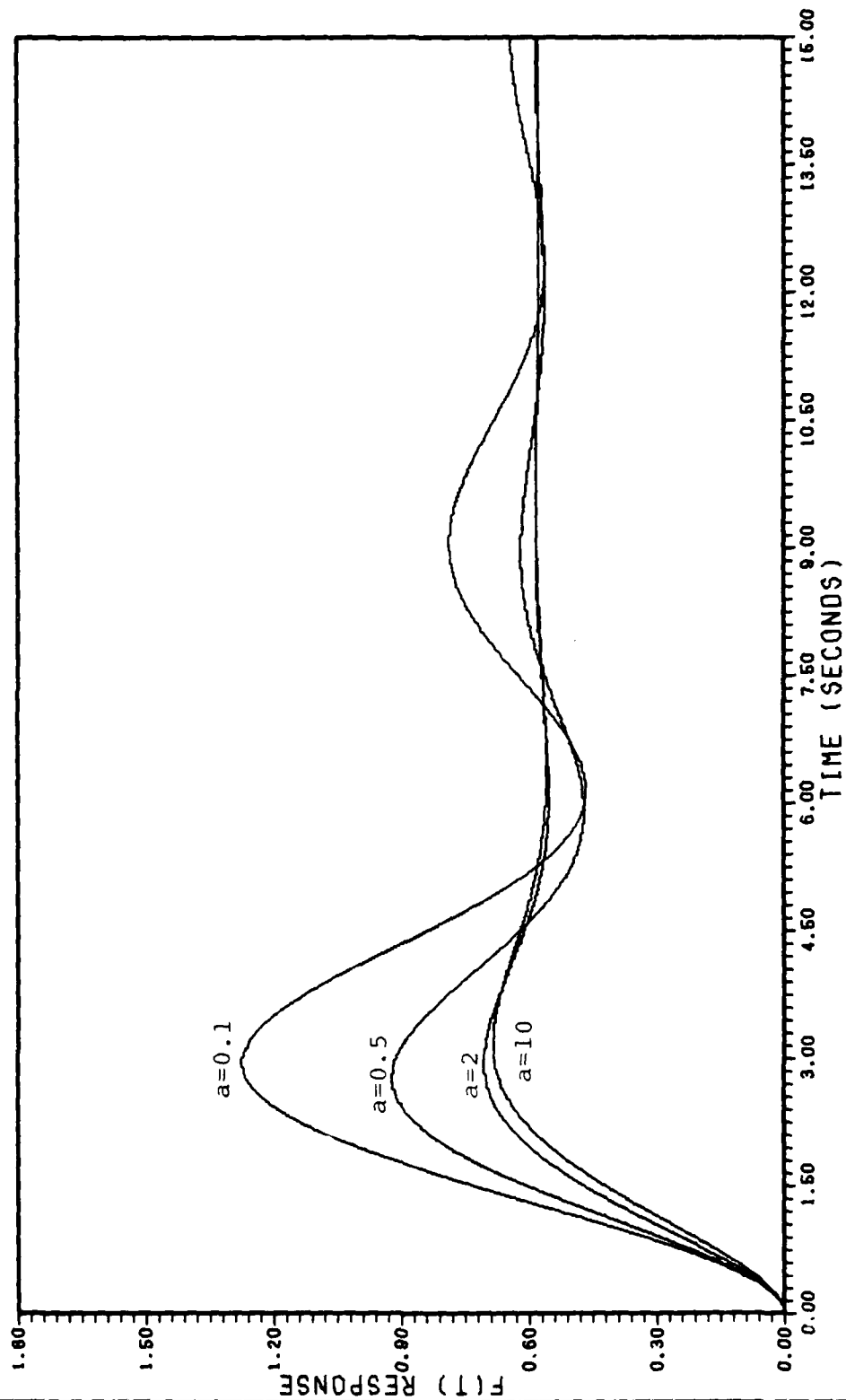
TIME RESPONSE FOR CASE E

Fig. 4-15. Time Responses for Case E

61

that this can be done with the following cost functionals
(Ref 7:5):

$$\underline{Q}(\omega) = \begin{bmatrix} \dfrac{a^4}{(\omega^2-a^2)^2} & 0 \\ 0 & \dfrac{a^4}{(\omega^2-a^2)^2} \end{bmatrix} \qquad (4-72)$$

$\underline{Q}(\omega)$ is factored into the following values of $\underline{P}_1^T(j\omega)$ and
$\underline{P}_1(j\omega)$

$$\underline{P}_1^T(j\omega) = \underline{P}_1(j\omega) = \begin{bmatrix} \dfrac{a^2}{\omega^2-a^2} & 0 \\ 0 & \dfrac{a^2}{\omega^2-a^2} \end{bmatrix} \qquad (4-73)$$

The controller system state equations for a minimal realization of the transfer between $\underline{x}^1(s)$ and $\underline{x}(s)$ are the
following:

$$\underline{\dot{z}}_1(t) = \begin{bmatrix} 0 & 1 \\ a^2 & 0 \end{bmatrix} \underline{z}_1(t) + \begin{bmatrix} 0 & 0 \\ a^2 & 0 \end{bmatrix} \underline{x}(t) \qquad (4-74)$$

$$\underline{x}^1(t) = \begin{bmatrix} 1 & 0 \\ 0 & 0 \end{bmatrix} \underline{z}_1(t) + \begin{bmatrix} 0 & 0 \\ 0 & 0 \end{bmatrix} \underline{x}(t) \qquad (4-75)$$

The augmented system equations are the following:

$$\underline{\dot{\tilde{x}}}(t) = \left[\begin{array}{cc:cc} 0 & 1 & 0 & 0 \\ -1 & -0.4 & 0 & 0 \\ \hdashline a & 0 & -a & 0 \\ 0 & a & 0 & -a \end{array}\right] \underline{\tilde{x}}(t) + \begin{bmatrix} 0 \\ 1 \\ 0 \\ 0 \end{bmatrix} u(t) \qquad (4-76)$$

The augmented system penalty matrices are defined by Eq
(4-43) to be the following:

62

$$\tilde{Q} = \begin{bmatrix} 0 & 0 & 0 & 0 \\ 0 & 0 & 0 & 0 \\ 0 & 0 & 1 & 0 \\ 0 & 0 & 0 & 0 \end{bmatrix} \qquad \tilde{R} = [1] \qquad\qquad (4\text{-}77)$$

Table 4-13 shows the characteristics for Case F. All of the systems are either poorly damped or have very small natural frequencies or both. Each system has two oscillatory modes except the system with $a = 10$.

Fig. 4-16 shows the Bode response characteristics of the system. As with all of the previous cases, the high-frequency response is the same as the open-loop system. As with Case D, the most significant result is that this frequency shaping can be used to reject low frequency disturbances. The frequency shaping only has an effect on disturbances or modes that are of lower frequency than the natural frequency of the closed-loop system. This result is achieved by removing the "a^4" constant in the numerator of the state cost functionals. The Bode plots shown in Fig. 4-16 describe systems with the constant "a^4" present, but when the constant is removed, the dc gain for the closed-loop system is very low for small values of "a".

The frequency response does not do anything particularly out of the ordinary near the natural frequency of the open-loop system. Gupta's premise that this type of weighting is good for supressing a disturbance at $\omega = a$ is not evident. Rather the controller is good at suppressing disturbances at frequencies less than the natural frequency.

63

Table 4-13. Characteristics of System F

| "a"	Riccati Feedback Gain, K	Closed-Loop Transfer Function Zeros	Poles	Natural Freq, ω_n	Damping Ratio, ζ	DC Gain
10	[220.1, 20.6, 222.5, 22.25]	10 −10	−0.493±1.08j −9.77 −10.2	1.19	0.414	0.708
5	[60.02, 10.56, 62.43, 12.48]	5 −5	−0.481±1.09j −4.99±0.076j	1.19	0.404	0.708
1	[3.59, 2.31, 6.01, 5.92]	1 −1	−0.283±1.05j −1.07±0.216j	1.09	0.260	0.708
0.5	[1.11, 1.42, 3.52, 6.76]	0.5 −0.5	−0.237±0.833j −0.675±0.130j	0.866	0.274	0.708
0.1	[0.112, 0.220, 2.53, 23.2]	0.1 −0.1	−0.110±0.045j −0.200±0.980j	0.119	0.93	0.708

64
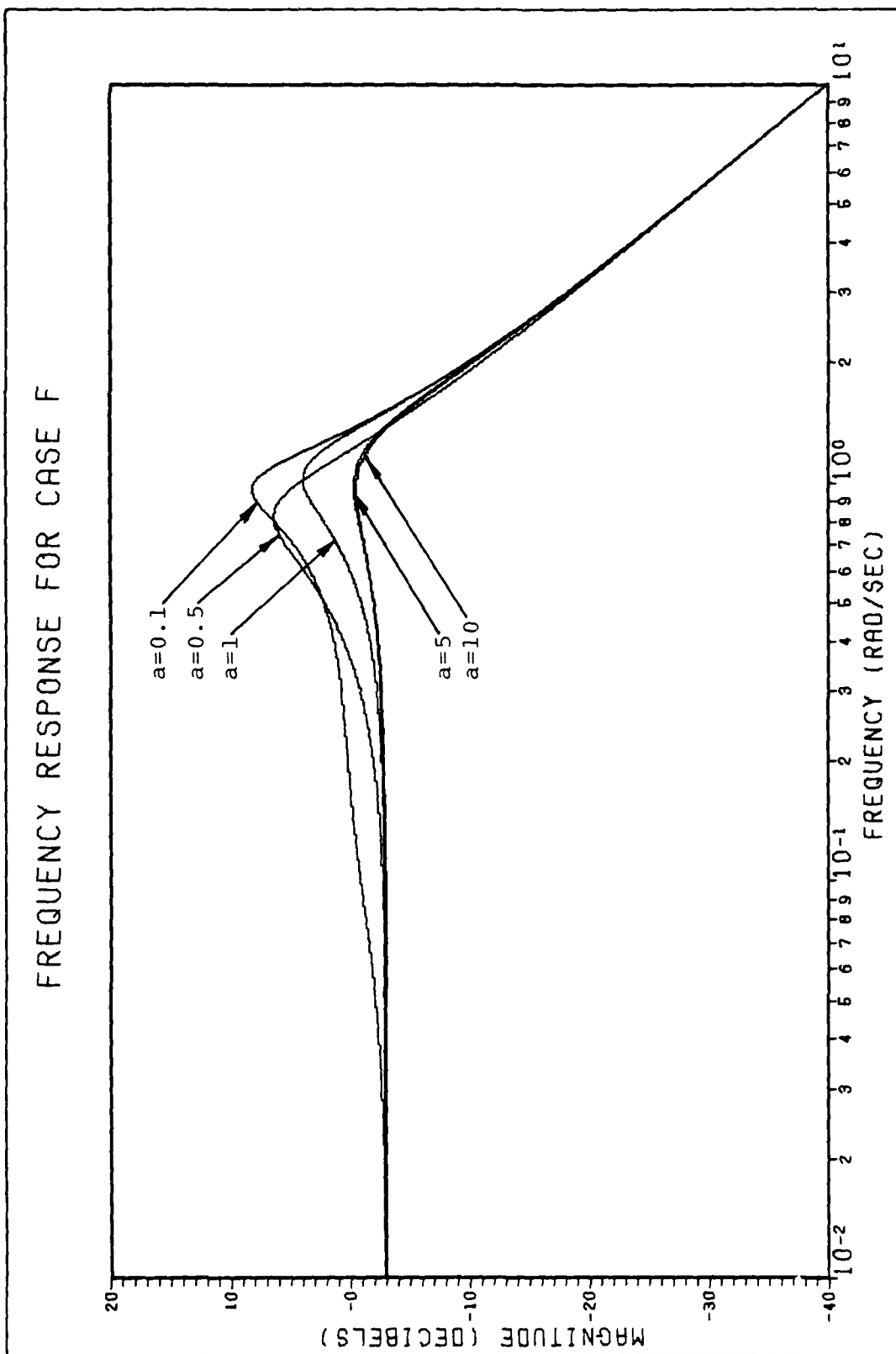
Fig. 4-16. Frequency Response for Case F.

65

Table 4-14 shows the time response characteristics for Case F. The systems with small values of "a" initially respond in the opposite direction of the final value. The low damping ratios for the systems are shown. The final value may be changed from -0.707 to 0.707 by multiplying the system closed-loop transfer function between $\underline{x}$(t) and u(t) by minus one. The settling times for this case are much larger than previous cases. Fig. 4-17 shows the time response for Case F.

Table 4-14.   Time Response Characteristics for Case F

"a"	Rise Time (sec)	Peak Time (sec)	Settling Time (sec)	Peak Value	Final Value
10	1.26	3.12	7.30	0.884	-0.707
5	1.25	3.30	7.47	0.884	-0.707
1	1.05	4.46	14.4	1.002	-0.707
0.5	1.02	5.84	18.43	1.097	-0.707
0.1	12.9	32.3	Very Large	0.723	-0.707

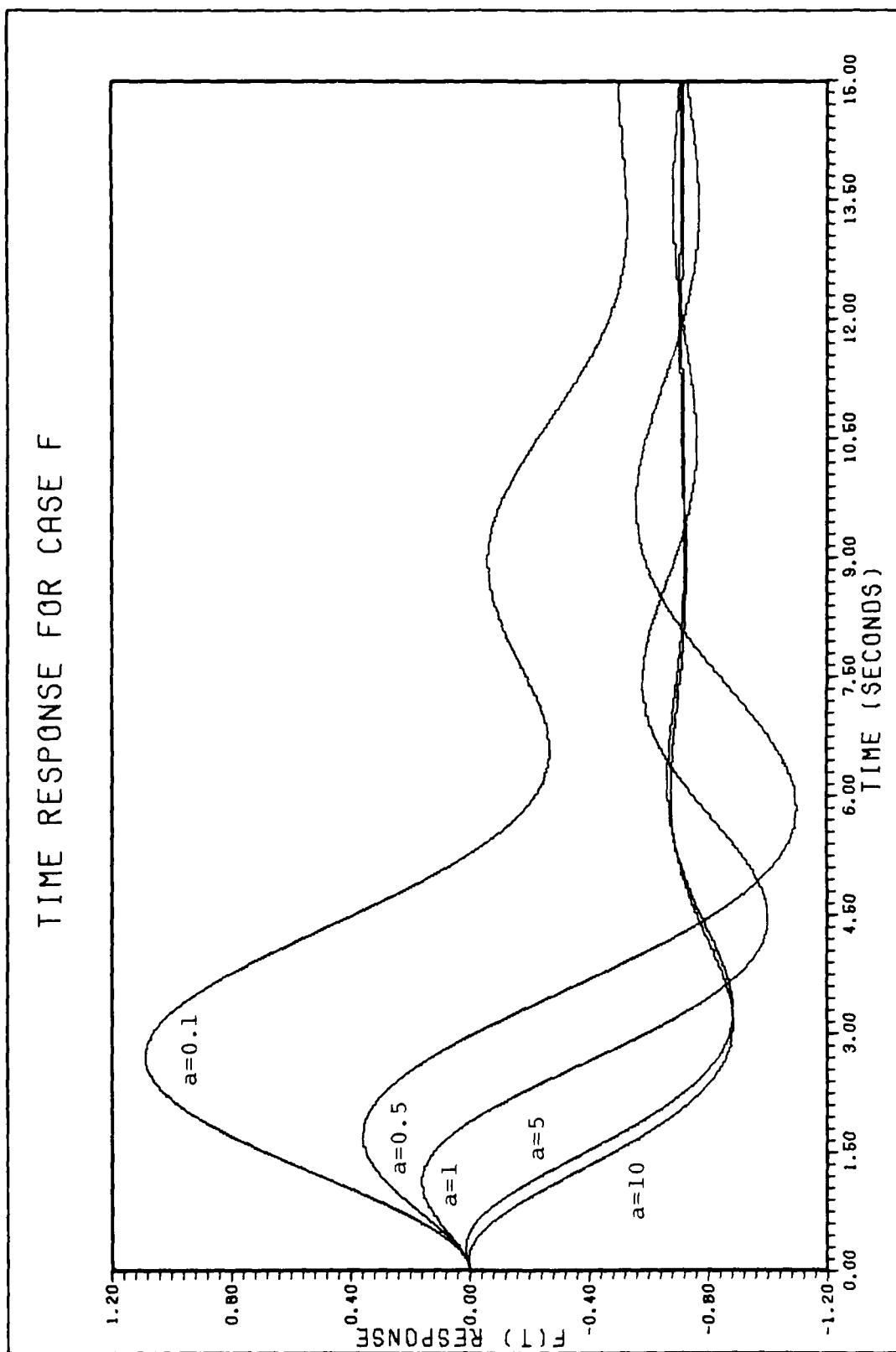TIME RESPONSE FOR CASE F

Fig. 4-17. Time Response for Case F

67

V Conclusions

Frequency shaping of quadratic cost functionals gives the control engineer additional flexibility in designing control systems, especially in suppressing low frequency modes and disturbances. Using appropriate values for the choice of compensator values of "a" and "b", the damping ratios can be significantly increased over the baseline open-loop system, thereby decreasing both overshoot and settling time. The baseline conventional controller has a larger value for the damping ratio than the frequency shaped controllers. This is because the latter has weighting matrix values that only approached the unity values of the baseline controller. However, the frequency shaped controllers demonstrate the ability to suppress rejections and system modes which occur at frequencies less than the natural frequency of the open-loop system. The rise time can also be reduced with the frequency shaped controllers. High frequency asymptotes had slopes of -40 db/decade for the baseline system and all of the controllers.

The controller with both numerator and denominator frequency weighting (s^2+a^2/s^2+b^2) demonstrated the most flexibility in achieving a variety of design character-istics. State penalty frequency weighting can be inter-preted as processing the state through a linear shaping filter. Control penalty frequency weighting is identical to incorporating control actuator dynamics into the system.

VI   Recommendations

Optimal control using frequency weighted cost functionals provides the designer with a wide spectrum of compensation characteristics. This method can improve the response of many control systems of interest to the Air Force, particularly in low frequency disturbance suppression. The effect of frequency shaping on the suppression of low frequency disturbances and system modes should be examined further.

Bibliography

1. Bryson, Arthur E., Jr., and Yu-Chi Ho. *Applied Optimal Control* (Revised Edition). Washington: Hemisphere Publishing Corporation, 1975.

2. Calico, Robert A., Jr. Lecture notes from MC6.28, Aircraft Control II. School of Engineering, Air Force Institute of Technology, Wright-Patterson Air Force Base, Ohio, 1981.

3. D'Azzo, John J. and Constantine H. Houpis. *Linear Control System Analysis and Design: Conventional and Modern*. New York: McGraw-Hill Book Company, 1975.

4. DiStefano, Joseph J., III, Allen R. Stubberud, and Ivan J. Williams. *Feedback and Control Systems*. New York: McGraw-Hill Book Company, 1967.

5. Fortmann, Thomas E. and Konrad L. Hitz. *An Introduction to Linear Control Systems*. New York: Marcel Dekker, Inc., 1977.

6. Gupta, Narendra K. "Frequency-Shaped Cost Functionals: Extension of Linear--Quadratic-Caussian Design Methods," *Journal of Guidance and Control*, 3 (6): 529-535 (November-December 1980).

7. Gupta, N. K., M. G. Lyons, J-N, Aubrun, and G. Margulies. *Frequency-Shaping Methods in Large Space Structures Control* (Symposium Paper for the 1981 Conference on Guidance and Control, Albuquerque, New Mexico).

8. Kirk, Donald E. *Optimal Control Theory*. Englewood Cliffs, New Jersey: Prentice-Hall, Inc., 1970.

9. Kleinman, David L. *Computer Programs Useful in Linear Systems Studies* (Revised Edition). Cambridge, Massachusetts: Heath and Dillow, 1974.

10. Larimer, Stanley J. *TOTAL: An Interactive Computer-Aided Design Program for Digital and Continuous Control System Analysis and Synthesis*. Thesis, Air Force Institute of Technology, Wright-Patterson Air Force Base, Ohio, 1978.

11. McRuer, Duane, Irving Ashkenas, and Dunstan Graham. *Aircraft Dynamics and Automatic Control*. Princeton, New Jersey: Princeton University Press, 1973.

12. Maybeck, Peter S. Lecture notes from EE7.12, Linear Estimation and Control. School of Engineering, Air Force Institute of Technology, Wright-Patterson Air Force Base, Ohio, 1981.

13. Maybeck, Peter S. Stochastic Models, Estimation, and Control, Volume 1. New York: Academic Press, 1979.

14. OPTCON: Optimal Control Design Program. Air Force Institute of Technology, Wright-Patterson Air Force Base, Ohio, 1974.

15. Silverthorn, James T. Lecture notes from MC7.28 Advanced Flight Mechanics and Aircraft Control. School of Engineering, Air Force Institute of Technology, Wright-Patterson Air Force Base, Ohio, 1981.

Appendix A   Calculation of Transfer Function Between
              $\underline{x}_1(s)$ and $\underline{u}_c(s)$ for Case E

$$\underline{\dot{x}}(t) = \underline{A}\underline{x}(t) + \underline{B}\underline{u}(t) + \underline{B}\underline{u}_c(t) \tag{A-1}$$

$$\underline{u}(s) = \frac{a\underline{\ddot{u}}(s)}{s+a} \tag{A-2}$$

$$\underline{\ddot{u}}(s) = K_1\underline{x}(s) + K_2\underline{u}(s) \tag{A-3}$$

$$\underline{u}(s) = -a\underline{u}(s) + a\underline{K}_1\underline{x}(s) + a\underline{K}_3\underline{u}(s) \tag{A-4}$$

$$(s\underline{I}-\underline{A})\underline{x}(s) = \underline{B}\underline{u}(s) + \underline{B}\underline{u}_c(c) \tag{A-5}$$

$$(s+a - aK_3)\underline{u}(s) = a\underline{K}_1\underline{x}(s) \tag{A-6}$$

$$\underline{u}(s) = \frac{a\underline{K}_1\underline{x}(s)}{(s+a - aK_3)} \tag{A-7}$$

$$(s\underline{I}-\underline{A})\underline{x}(s) = \frac{\underline{B}\,a\underline{K}_1\underline{x}(s)}{(s+a - aK_3)} + \underline{B}\,\underline{u}_c(s) \tag{A-8}$$

$$\left[(s\underline{I}-\underline{A}) - \frac{\underline{B}a\,\underline{K}_1}{(s+a - aK_3)}\right]\underline{x}(s) = \underline{B}\,\underline{u}_c(s) \tag{A-9}$$

$$\underline{x}(s) = \left[(s\underline{I}-\underline{A}) - \frac{\underline{B}a\,\underline{K}_1}{(s+a - aK_3)}\right]^{-1}\underline{B}\,\underline{u}_c(s) \tag{A-10}$$

$$H(s) = \frac{\underline{x}(s)}{\underline{u}_c(s)} = \left[(s\underline{I}-\underline{A}) - \frac{\underline{B}a\,\underline{K}_1}{(s+a - aK_3)}\right]^{-1}\underline{B} \tag{A-11}$$

here $\underline{A} = \begin{bmatrix} 0 & 1 \\ -1 & -0.4 \end{bmatrix}$, $\underline{B} = \begin{bmatrix} 0 \\ 1 \end{bmatrix}$, $a = [a]$ (A-12)

$$\underline{K}_1 = [K_1 \ K_2] \quad K_3 = K_3 \tag{A-13}$$

Substituting in the values of the matrices we get the
following:

72

$$\underline{H}(s) = \left\{ \begin{bmatrix} S & -1 \\ 1 & S+0.4 \end{bmatrix} - \begin{bmatrix} 0 & 0 \\ \dfrac{aK_1}{s+a - aK_3} & \dfrac{aK_2}{s+a - aK_3} \end{bmatrix} \right\}^{-1} \begin{array}{c} 0 \\ 1 \end{array} \quad \text{(A-14)}$$

$$\underline{H}(s) = \left\{ \begin{bmatrix} S & -1 \\ \dfrac{(s+a - aK_3)}{(s+a - aK_3)} & \dfrac{(s+0.4)(s+a - aK_3)}{(s+a - aK_3)} \end{bmatrix} \right.$$

$$\left. - \begin{bmatrix} 0 & 0 \\ \dfrac{aK_1}{(s+a - aK_3)} & \dfrac{aK_2}{(s+a - aK_3)} \end{bmatrix} \right\}^{-1} \begin{bmatrix} 0 \\ 1 \end{bmatrix} \quad \text{(A-15)}$$

$$\underline{H}(s) = \begin{bmatrix} S & -1 \\ \dfrac{(s+a - aK_1 - aK_3)}{(s+a - aK_3)} & \dfrac{(s+0.4)(s+a - aK_3)-aK_2}{(s+a - aK_3)} \end{bmatrix}^{-1} \begin{bmatrix} 0 \\ 1 \end{bmatrix} \quad \text{(A-16)}$$

$$\underline{H}(s) = \dfrac{(s+a - aK_3)}{s[(s+0.4)(s+a - aK_3) - aK_2] + (s+a - aK_3 - aK_1)} \times$$

$$\begin{bmatrix} \dfrac{(s+0.4)(s+a - aK_3) - aK_2}{s+a - aK_3} & +1 \\ \dfrac{-(s+a - aK_3 - aK_1)}{s+a - aK_3} & S \end{bmatrix} \begin{bmatrix} 0 \\ 1 \end{bmatrix} \quad \text{(A-17)}$$

$$\underline{H}(s) = \begin{bmatrix} \dfrac{(s+a - aK_3)}{s[(s+0.4)(s+a - aK_3) - aK_2] + (s+a - aK_3 - aK_1)} \\ \dfrac{-(s+a - aK_3)}{[(s+0.4)(s+a - aK_3) - aK_2] + (s+a - aK_3 - aK_1)} \end{bmatrix} \quad \text{(A-18)}$$

73

Appendix B   <u>Creating</u> <u>a</u> <u>Realization</u> <u>for</u> <u>a</u> <u>System</u>

Fortman and Hitz discuss the procedure of generating
a realization in detail (Ref 4:441-451). Briefly, the
goal is to find the system equations

$$\underline{\dot{x}}(t) = \underline{A}\underline{x}(t) + \underline{B}\underline{u}(t) \tag{B-1}$$

$$\underline{y}(t) = \underline{C}\underline{x}(t) + \underline{D}\underline{u}(t) \tag{B-2}$$

that realize a system transfer function matrix, $\underline{H}(s)$
where

$$\underline{H}(s) = \underline{C}(s\underline{I}-\underline{A})^{-1}\underline{B} + \underline{D} \tag{B-3}$$

In general, the realization will not be unique. If the
state, $\underline{x}(s)$, the control $\underline{u}(s)$, and the output, $\underline{y}(s)$ have
dimensions n, m, and p respectively, then $\underline{H}(s)$ will be
a p x m transfer function matrix. The first step in
creating a realization is to express the transfer function
matrix in a ratio of polynomials in s, that is:

$$\underline{H}(s) = \frac{\underline{Q}_o + \underline{Q}_1 s + \underline{Q}_2 s^2 + \cdots \underline{Q}_{n-1} s^{n-1}}{P_o + P_1 s + P_2 s^2 + \cdots P_{n-1} s^{n-1} + s^n} \tag{B-4}$$

Note that Eq (B-4) is a proper transfer function. The
degree of the numerator is less than the denominator.
For cases involving improper transfer functions, the
polynomial equation must include a feed forward matrix,
$\underline{D}$.

$$\underline{H}(s) = \frac{\underline{Q}_0 + \underline{Q}_1(s) + \cdots \underline{Q}_{n-1} s^{n-1}}{p_0 + p_1(s) + \cdots p_{n-1} s^{n-1} + s^n} \qquad \text{(B-5)}$$

Appendix D illustrates the use of the feed forward matrix in improper transfer functions.

The next step is to describe the system in control canonical form using the p_i and $\underline{Q}_i$ values from Eq (B-4) or (B-5).

$$\underline{\dot{x}} = \begin{bmatrix} \underline{0}m & \underline{I}m & \underline{0}m & \cdots & \underline{0}m \\ \underline{0}m & \underline{0}m & \underline{I}m & \cdots & \underline{0}m \\ \cdot & & & & \cdot \\ \cdot & & & & \cdot \\ \cdot & & & & \cdot \\ \underline{0}m & \underline{0}m & \underline{0}m & \cdots & \underline{I}m \\ -p_0\underline{I}m & -p_1\underline{I}m & -p_2\underline{I}m & \cdots & -p_{n-1}\underline{I}m \end{bmatrix} \underline{x} + \begin{bmatrix} \underline{0}m \\ \underline{0}m \\ \cdot \\ \cdot \\ \cdot \\ \underline{0}m \\ \underline{I}m \end{bmatrix} \underline{u} \qquad \text{(B-6)}$$

$$\underline{y} = [\underline{Q}_0 \ \underline{Q}_1 \ \underline{Q}_2 \ \cdots \ \underline{Q}_{n-1}]\underline{x} \qquad \text{(B-7)}$$

The submatrices are of dimension m x m, denoted by the m subscript. While this method will provide a realization, in general, it will not be the minimal realization. In forming the plant matrix in Eq (B-6), the designer should fill in the lower left element first. Then the rest of the matrix elements should be filled as necessary to achieve the correct matrix dimension.

The final step is to find the minimal realization. A minimal system is both completely controllable and observable. The minimal realization can generally be found by starting in the upper left corner of the $\underline{A}$ matrix

and reducing $\tilde{A}$ to the dimension of the controllability matrix.

Appendix C Formation of Realization and
Transfer Function for Case C

$$\underline{P}_1(j\omega) = \begin{bmatrix} \dfrac{a}{j\omega+a} & 0 \\ \\ 0 & \dfrac{a}{j\omega+a} \end{bmatrix} \tag{C-1}$$

$$\underline{H}(s) = \frac{\underline{Q}_0 + \underline{Q}_1 s + \dots \underline{Q}_{n-1} s^{n-1}}{p_0 + p_1 s + \dots p_{n-1} s^{n-1} + s^n} \tag{C-2}$$

$$\underline{H}(s) = \frac{\begin{bmatrix} a & 0 \\ 0 & a \end{bmatrix}}{a + (1)s} \tag{C-3}$$

$$\underline{Q}_0 = \begin{bmatrix} a & 0 \\ 0 & a \end{bmatrix} \quad p_0 = a \tag{C-4}$$

$$\underline{\dot{z}}_1(t) = \underline{A}_1 \underline{z}_1(t) + \underline{B}_1 \underline{x}(t) \tag{C-5}$$

$$\underline{x}^1(t) = \underline{C}_1 \underline{z}_1(t) + \underline{D}_1 \underline{x}(t) \tag{C-6}$$

$$\underline{\dot{z}}_1(t) = [-p_0 I_2] \, \underline{z}_1(t) + [I_2] \, \underline{x}(t) \tag{C-7}$$

$$\underline{x}^1(t) = [\underline{Q}_0] \, \underline{Z}_1(t) \tag{C-8}$$

$$\underline{\dot{z}}_1(t) = \begin{bmatrix} -a & 0 \\ 0 & -a \end{bmatrix} \underline{z}_1(t) + \begin{bmatrix} 1 & 0 \\ 0 & 1 \end{bmatrix} \underline{x}(t) \tag{C-9}$$

$$\underline{x}^1(t) = \begin{bmatrix} a & 0 \\ 0 & a \end{bmatrix} \underline{z}_1(t) + \begin{bmatrix} 0 & 0 \\ 0 & 0 \end{bmatrix} \underline{x}(t) \tag{C-10}$$

$$\underline{P}_1(s) = \underline{C}_1 (s\underline{I} - \underline{A}_1)^{-1} \underline{B}_1 + \underline{D}_1 \tag{C-11}$$

$$\underline{P}_1(s) = \begin{bmatrix} a & 0 \\ 0 & a \end{bmatrix} \begin{bmatrix} s+a & 0 \\ 0 & s+a \end{bmatrix}^{-1} \begin{bmatrix} 1 & 0 \\ 0 & 1 \end{bmatrix} + \begin{bmatrix} 0 & 0 \\ 0 & 0 \end{bmatrix} \tag{C-12}$$

$$\underline{P}_1(s) = \frac{1}{(s+a)^2} \begin{bmatrix} a & 0 \\ 0 & a \end{bmatrix} \begin{bmatrix} s+a & 0 \\ 0 & s+a \end{bmatrix} \begin{bmatrix} 1 & 0 \\ 0 & 1 \end{bmatrix} \tag{C-13}$$

$$\underline{P}_1(s) = \begin{bmatrix} a & 0 \\ 0 & a \end{bmatrix} \begin{bmatrix} \frac{1}{s+a} & 0 \\ 0 & \frac{1}{s+a} \end{bmatrix} \tag{C-14}$$

$$\underline{P}_1(s) = \begin{bmatrix} \frac{1}{s+a} & 0 \\ 0 & \frac{1}{s+a} \end{bmatrix} \tag{C-15}$$

There are several possible realizations for a system given some transfer function. The realization described by Eqs (C-9) and (C-10) is not exactly the same as the realization which is used for Case C. Both realizations define $\underline{P}_1(j\omega)$, given by Eq (C-1).

Appendix D Formation of Realization and
Transfer Function for Case D

$$\underline{P}_1(j\omega) = \begin{bmatrix} \dfrac{j\omega+a}{j\omega+b} & 0 \\ 0 & \dfrac{j\omega+a}{j\omega+b} \end{bmatrix} \qquad\qquad\qquad \text{(D-1)}$$

$$\underline{P}_1(s) = \frac{\underline{Q}_0 + \underline{Q}_1(s) + \ldots \underline{Q}_{n-1}\, s^{n-1}}{p_0 + p_1(s) + \ldots + p_{n-1}\, s^{n-1} + s^n} + \underline{D} \quad \text{(D-2)}$$

$$\underline{P}_1(s) = \frac{\begin{bmatrix} a & 0 \\ 0 & a \end{bmatrix}}{b + (1)s} + \begin{bmatrix} 1 & 0 \\ 0 & 1 \end{bmatrix} = \frac{\begin{bmatrix} s+a & 0 \\ 0 & s+a \end{bmatrix}}{s + b} + \begin{bmatrix} 1 & 0 \\ 0 & 1 \end{bmatrix} \quad \text{(D-3)}$$

$$\underline{Q}_0 = \begin{bmatrix} a & 0 \\ 0 & a \end{bmatrix} \quad p_0 = b \qquad\qquad\qquad \text{(D-4)}$$

$$\underline{\dot{z}}_1(t) = [-p_0 I_2]\, \underline{z}_1(t) + [I_2]\, \underline{x}(t) \qquad\qquad \text{(D-5)}$$

$$\underline{x}^1(t) = [\underline{Q}_0]\underline{z}_1(t) + \begin{bmatrix} 1 & 0 \\ 0 & 1 \end{bmatrix} \underline{x}(t) \qquad\qquad \text{(D-6)}$$

$$\underline{\dot{z}}_1 = \begin{bmatrix} -b & 0 \\ 0 & -b \end{bmatrix} \underline{z} + \begin{bmatrix} 1 & 0 \\ 0 & 1 \end{bmatrix} \underline{x} \qquad\qquad \text{(D-7)}$$

$$\underline{x}^1 = \begin{bmatrix} a-b & 0 \\ 0 & a-b \end{bmatrix} \underline{z} + \begin{bmatrix} 1 & 0 \\ 0 & 1 \end{bmatrix} \underline{x} \qquad\qquad \text{(D-8)}$$

$$\underline{P}_1(s) = \underline{C}_1(s\underline{I} - \underline{A}_1)^{-1}\, \underline{B}_1 + \underline{D}_1 \qquad\qquad \text{(D-9)}$$

$$\underline{P}_1(s) = \begin{bmatrix} a-b & 0 \\ 0 & a-b \end{bmatrix} \begin{bmatrix} s+b & 0 \\ 0 & s+b \end{bmatrix}^{-1} \begin{bmatrix} 1 & 0 \\ 0 & 1 \end{bmatrix} + \begin{bmatrix} 1 & 0 \\ 0 & 1 \end{bmatrix} \quad \text{(D-10)}$$

$$\underline{P}_1(s) = \begin{bmatrix} a-b & 0 \\ 0 & a-b \end{bmatrix} \begin{bmatrix} \dfrac{1}{s+b} & 0 \\ 0 & \dfrac{1}{s+b} \end{bmatrix} \begin{bmatrix} 1 & 0 \\ 0 & 1 \end{bmatrix} + \begin{bmatrix} 1 & 0 \\ 0 & 1 \end{bmatrix} \quad \text{(D-11)}$$

$$\underline{P}_1(s) = \begin{bmatrix} \dfrac{a-b}{s+b} & 0 \\ 0 & \dfrac{a-b}{s+b} \end{bmatrix} + \begin{bmatrix} 1 & 0 \\ 0 & 1 \end{bmatrix} \qquad\qquad \text{(D-12)}$$

$$\underline{P}_1(s) = \begin{bmatrix} \dfrac{a-b}{s+b} & 0 \\ 0 & \dfrac{a-b}{s+b} \end{bmatrix} + \begin{bmatrix} \dfrac{s+b}{s+b} & 0 \\ 0 & \dfrac{s+b}{s+b} \end{bmatrix} \qquad\qquad \text{(D-13)}$$

$$\underline{P}_1(s) = \begin{bmatrix} \dfrac{s+b-b+a}{s+b} & 0 \\ 0 & \dfrac{s+b-b+a}{s+b} \end{bmatrix} = \begin{bmatrix} \dfrac{s+b}{s+b} & 0 \\ 0 & \dfrac{s+a}{s+b} \end{bmatrix} \qquad\qquad \text{(D-14)}$$

VITA

   D. V. Palmer attended high school in Denver, Colorado.
After graduating from the United States Air Force Academy
with an engineering degree, he received his commission
in the United States Air Force. He worked as an aero-
nautical engineer at Edwards Air Force Base and entered
the Graduate Aeronautical Engineering Program at AFIT in
1980.

          Permanent address: 419 Lake Topaz Cres SE
                              Calgary, Alberta T2J-2H7
                              Canada

REPORT DOCUMENTATION PAGE		READ INSTRUCTIONS BEFORE COMPLETING FORM
1. REPORT NUMBER AFIT/GAE/AA/81D-22	2. GOVT ACCESSION NO.	3. RECIPIENT'S CATALOG NUMBER
4. TITLE (and Subtitle) Optimal Control Using Frequency Weighted Cost Functionals		5. TYPE OF REPORT & PERIOD COVERED MS Thesis
		6. PERFORMING ORG. REPORT NUMBER
7. AUTHOR(s) D. V. Palmer Capt USAF		8. CONTRACT OR GRANT NUMBER(s)
9. PERFORMING ORGANIZATION NAME AND ADDRESS Air Force Institute of Technology (AFIT-EN) Wright Patterson AFB, Ohio 45433		10. PROGRAM ELEMENT, PROJECT, TASK AREA & WORK UNIT NUMBERS
11. CONTROLLING OFFICE NAME AND ADDRESS		12. REPORT DATE December
		13. NUMBER OF PAGES 81
14. MONITORING AGENCY NAME & ADDRESS(if different from Controlling Office)		15. SECURITY CLASS. (of this report) Unclassified
		15a. DECLASSIFICATION DOWNGRADING SCHEDULE

16. DISTRIBUTION STATEMENT (of this Report)

Approved for public release; distribution unlimited.

17. DISTRIBUTION STATEMENT (of the abstract entered in Block 20, if different from Report)

Air Force Institute of Technology (ATC)
Wright-Patterson AFB, OH 45433

FREDRIC C. LYNCH, Major, USAF
Director of Public Affairs

18. SUPPLEMENTARY NOTES

Approved for public release; IAW 190-17

Frederic C. Lynch, Major, USAF
Director of Public Affairs

28 JAN 1982

19. KEY WORDS (Continue on reverse side if necessary and identify by block number)

Optimal Control   Linear Quadratic Regulator
Frequency Weightings
Cost Functionals
Modern Control

20. ABSTRACT (Continue on reverse side if necessary and identify by block number)

A simple lightly damped second-order system is augmented with an optimal controller using linear quadratic regulator theory. However, instead of using conventional optimal control design methods, the controller is designed with frequency weighted cost functionals. This report investigates the effect of frequency shaping on the frequency and time response characteristics of the closed-loop system.

20.

The effects of frequency shaping on the state and control
penalty matrices are analyzed separately. Each test case yields
improved damping ratios compared with the baseline open-loop
system. Each system, including the baseline model, has a high
frequency asymptote slope of -40 dB/decade. There is very
little difference in the high-frequency response characteristics
of the frequency shaped augmented systems and the open-loop
system.

The most important result is that the low frequency magni-
tude response can be reduced by using frequency shapings. This
is particularly useful in attenuating low frequency system modes
as well as low frequency noise.

END

DATE
FILMED

03-82

DTIC